

AD-A204 047

INTATION PAGE

Form Approved
OMB No. 0704-0188

1a. REPORT TYPE AND DATES COVERED Unclassified		1b. RESTRICTIVE MARKINGS DTIC FILE COPY										
2a. SECURITY CLASSIFICATION AUTHORITY		3. DISTRIBUTION/AVAILABILITY OF REPORT Approved for public release; distribution is unlimited										
2b. DECLASSIFICATION/DOWNGRADING SCHEDULE		5. MONITORING ORGANIZATION REPORT NUMBER(S) AFOSR-TR-89-0010										
4. PERFORMING ORGANIZATION REPORT NUMBER(S)		7a. NAME OF MONITORING ORGANIZATION AFOSR/NA										
6a. NAME OF PERFORMING ORGANIZATION Rensselaer Polytechnic Inst.	6b. OFFICE SYMBOL (if applicable) Chemical Eng.	7b. ADDRESS (City, State, and ZIP Code) Building 410, Bolling AFB DC 20332-6448										
6c. ADDRESS (City, State, and ZIP Code) Troy, NY 12180-3590		9. PROCUREMENT INSTRUMENT IDENTIFICATION NUMBER AFOSR 86-0019										
8a. NAME OF FUNDING/SPONSORING ORGANIZATION AFOSR/NA	8b. OFFICE SYMBOL (if applicable) NA	10. SOURCE OF FUNDING NUMBERS										
8c. ADDRESS (City, State, and ZIP Code) Building 410, Bolling AFB DC 20332-6448		PROGRAM ELEMENT NO. 61102F	TASK NO. A1									
11. TITLE (Include Security Classification) (U) Advanced B and A1 Combustion Kinetics Over Wide Temperature Ranges		PROJECT NO. 2308	WORK UNIT ACCESSION NO. 10 FEB 1989									
12. PERSONAL AUTHOR(S) Arthur Fontijn		15. PAGE COUNT 62										
13a. TYPE OF REPORT Final	13b. TIME COVERED FROM 12/1/85 TO 11/30/88	14. DATE OF REPORT (Year, Month, Day) 1989 January 19										
16. SUPPLEMENTARY NOTATION												
17. COSATI CODES		18. SUBJECT TERMS (Continue on reverse if necessary and identify by block number)										
FIELD	GROUP	<table border="1"> <tr> <td>Combustion Kinetics</td> <td>Ramjets</td> <td>A10</td> </tr> <tr> <td>High Temperature</td> <td>A1</td> <td>BC1</td> </tr> <tr> <td>Solid Rocket Propulsion</td> <td>A1C1</td> <td>Radiative Lifetimes</td> </tr> </table>		Combustion Kinetics	Ramjets	A10	High Temperature	A1	BC1	Solid Rocket Propulsion	A1C1	Radiative Lifetimes
Combustion Kinetics	Ramjets	A10										
High Temperature	A1	BC1										
Solid Rocket Propulsion	A1C1	Radiative Lifetimes										
19. ABSTRACT (Continue on reverse if necessary and identify by block number) To help provide a better understanding of the temperature dependence of the kinetics of gas-phase metal oxidation reactions, experimental measurements were made in the 440 to 1830 K temperature regime using a high-temperature fast-flow reactor (HTFFR). The relative concentrations of the metallic species were monitored by visible/uv laser-induced fluorescence. The following rate coefficient expressions were obtained (in cubic cm, per molecule, per second units): $Al + Cl(2) \rightarrow AlCl + Cl$, $7.9 \times 10(-10) \exp(-780 K/T)$; $Al + HCl \rightarrow AlCl + H$, $1.5 \times 10(-10) \exp(-800 K/T)$; <p style="text-align: right;">Continued on back.....</p>												
20. DISTRIBUTION/AVAILABILITY OF ABSTRACT <input checked="" type="checkbox"/> UNCLASSIFIED/UNLIMITED <input checked="" type="checkbox"/> SAME AS RPT <input checked="" type="checkbox"/> DTIC USERS		21. ABSTRACT SECURITY CLASSIFICATION Unclassified										
22a. NAME OF RESPONSIBLE INDIVIDUAL Dr Mitat Birkan		22b. TELEPHONE (Include Area Code) (202) 767-4938	22c. OFFICE SYMBOL AFOSR/NA									

19. Abstract (continued)

$\text{AlCl} + \text{Cl}(2) \rightarrow \text{AlCl}(2) + \text{Cl}$, $9.6 \times 10^{-11} \exp(-610 \text{ K/T})$; $\text{AlCl} + \text{CO}(2) \rightarrow \text{OAlCl} + \text{CO}$, $2.5 \times 10^{-12} \exp(-7550 \text{ K/T})$; $\text{AlCl} + \text{O}(2) \rightarrow \text{products}$, $1.3 \times 10^{-12} \exp(-3400 \text{ K/T}) + 3.4 \times 10^{-9} \exp(-16100 \text{ K/T})$; $\text{AlO} + \text{Cl}(2) \rightarrow \text{OAlCl} + \text{Cl}$, $3.0 \times 10^{-10} \exp(-1250 \text{ K/T})$; $\text{AlO} + \text{HCl} \rightarrow \text{OAlCl} + \text{H}$, $5.6 \times 10^{-11} \exp(-140 \text{ K/T})$; $\text{BCl} + \text{O}(2) \rightarrow \text{Products}$, $2.2 \times 10^{-11} \exp(-4620 \text{ K/T})$; $\text{BCl} + \text{CO}(2) \rightarrow \text{OBCl} + \text{CO}$, $1.8 \times 10^{-31} T^{5.6} \exp(-1190 \text{ K/T})$.

These B and Al results are compared. Existing theory is found to be inadequate to describe or predict these results. To allow, in future work, identification of some of the tri-atomic products, which do not have identified electronic spectra, a second HTFFR facility was built. In it the Al and B species are monitored by mass spectrometry.

The radiative lifetime of AlCl (A one pie), of importance to plume models, was determined by 6.4 ns.

DISCLAIMER NOTICE

**THIS DOCUMENT IS BEST QUALITY
PRACTICABLE. THE COPY FURNISHED
TO DTIC CONTAINED A SIGNIFICANT
NUMBER OF PAGES WHICH DO NOT
REPRODUCE LEGIBLY.**

**BEST
AVAILABLE COPY**

TABLE OF CONTENTS

	<u>Page</u>
I. RESEARCH OBJECTIVES	1
II. RESULTS	2
A. Cumulative Chronological List of Publications	2
B. Partially Completed Studies	6
C. Some General Observations	8
III. PROFESSIONAL PERSONNEL	9
IV. PRESENTATIONS AND OTHER INTERACTIONS	9

APPENDIX 1 - D.F. Rogowski and A. Fontijn, "An HTFFR Kinetics Study of the Reaction Between AlCl and O₂ from 490 to 1750 K", Twenty-first Symposium (International) on Combustion, The Combustion Institute, Pittsburgh, 1986, pp. 943-952.

APPENDIX 2. - D.F. Rogowski and A. Fontijn, "An HTFFR Kinetics Study of the Reaction Between AlCl and CO₂ from 1175 to 1775 K", *Chemical Physics Letters*, 132, 413-416 (1986).

APPENDIX 3. -D.F. Rogowski and A. Fontijn, "The Radiative Lifetime of AlCl A¹I", *Chemical Physics Letters*, 137, 219-222 (1987).

APPENDIX 4. - A.G. Slavejkov, D.F. Rogowski and A. Fontijn, "An HTFFR Kinetics Study of the Reaction Between BCl and O₂ from 540 to 1670 K", *Chemical Physics Letters*, 143, 26-30 (1988).

APPENDIX 5. - D.F. Rogowski, P. Marshall and A. Fontijn, "High-Temperature Fast-Flow Reactor (HTFFR) Kinetics Studies of the Reactions of Al with Cl₂, Al with HCl and AlCl with Cl₂ Over Wide Temperature Ranges", *The Journal of Physical Chemistry*, in press.



Accession For	
NTIS GRA&I	<input checked="" type="checkbox"/>
DTIC TAB	<input type="checkbox"/>
Unannounced	<input type="checkbox"/>
Justification	
By _____	
Distribution/	
Availability Codes	
Dist	Avail and/or Special
A-1	

I. RESEARCH OBJECTIVES

Current ability to transfer engineering data, on rocket chamber and plume combustion, from present to advanced propulsion systems is hampered by a lack of understanding and knowledge of individual A1 and B species reactions and the ways by which temperature affects the reaction rate coefficients. The Arrhenius equation $k(T) = A \exp(-E/RT)$ has over limited temperature ranges been of great value. However, over the large temperature ranges of interest to rocket propulsion systems, order of magnitude errors can be made by extrapolations based on it, particularly for exothermic and slightly endothermic reactions.* Other $k(T)$ expressions and current theory are inadequate to predict or describe the observations made thus far for reactions of metallic propellant species.

The goals of the work reported have been to provide, through accurate measurements, reliable data on, and improved insight into, the kinetic behavior of A1 and B atom, monohalide and monoxide radical oxidation reactions, as influenced by temperature. The measurements have been made using the HTFFR (high-temperature fast-flow reactor) technique. HTFFRs are unique tools, which provide measurements on isolated elementary reactions in a heat bath. With traditional high-temperature techniques, such as flames and shock tubes, such isolation is usually impossible to achieve; as a result, data on any given reaction depend on the knowledge of other reactions occurring simultaneously, leading to large uncertainties. HTFFRs allow kinetic studies from room temperature up to about 1900 K to provide wide range $k(T)$ (temperature-dependent rate coefficient) data. In the work reported, laser-induced fluorescence LIF has been used to monitor the metallic atom or radical reactant concentrations, as a function

*A Fontijn and R. Zellner, "Influence of Temperature on Rate Coefficients of Bimolecular Reactions," Reactions of Small Transient Species. Kinetics and Energetics, A. Fontijn and M.A.A. Clyne, Eds., (Academic Press, London, 1983), Chap. 1.

of time, concentration of the molecular oxidant (present in excess), temperature and pressure.

Most tri-atomic products of the oxidation reactions of the monoxides and monohalides have no identified electronic transition spectra and cannot be detected by LIF. To unambiguously establish the kinetics of reactions involving these tri-atomics and ultimately to develop a good understanding of the reactions leading to the final combustion products, Al_2O_3 and B_2O_3 , we have under the present grant constructed an HTFFR with mass spectrometer detection. Measurements with this new facility are to be performed under a follow-up grant.

These general objectives and a systematic of the experimental facilities are illustrated in Fig. 1.

II. RESULTS

In Fig. 2 our rate coefficient measurements for Al system reactions are summarized. In Fig. 3 we summarize the first results on B system (thus far BCl) reactions. Some of these studies preceded the present grant. Those that were made and published under this grant are listed in Section II.A.. In Section II.B. we discuss the results that are in the process of being written up or are being completed under the follow-up grant, while in Section II.C. we make a few additional remarks about the implications of our findings.

A. Cumulative Chronological List of Publications

1. D.F. Rogowski and A. Fontijn, "An HTFFR Kinetics Study of the Reaction Between AlCl and O_2 from 490 to 1750 K", Twenty-first Symposium (International) on Combustion, The Combustion Institute, Pittsburgh, 1986, pp. 943-952.
2. D.F. Rogowski and A. Fontijn, "An HTFFR Kinetics Study of the Reaction Between AlCl and CO_2 from 1175 to 1775 K", *Chemical Physics Letters*, 132, 413-416 (1986).

Figure 1

AIR FORCE BASIC RESEARCH

SCIENTIFIC APPROACH

PROBLEM

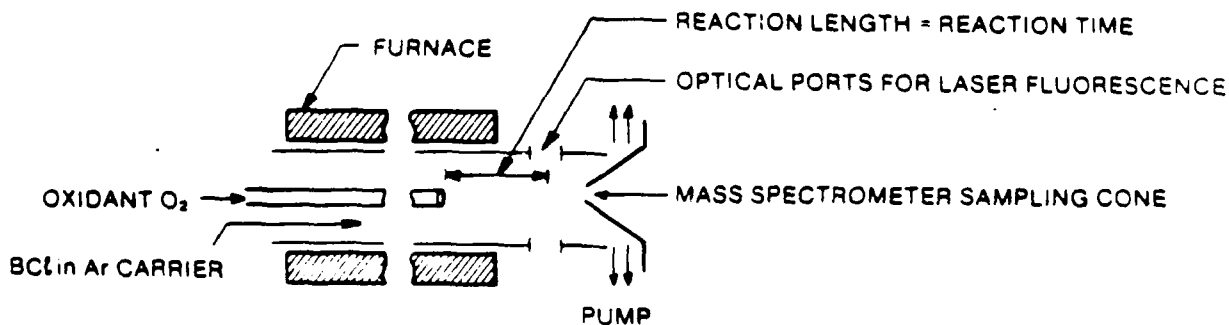
- CURRENT MODELS OF B AND Al COMBUSTION IN ROCKET MOTORS AND EXHAUSTS LACK RELIABLE CHEMICAL KINETIC INPUT DATA, WHICH HAMPERS DEVELOPMENT OF ADVANCED SYSTEMS.

GOALS

- OBTAIN KINETIC DATA OVER THE 300-1,900 K RANGE. CHANGING MECHANISMS AND NON-ARRHENIUS BEHAVIOR PRECLUDE EXTRAPOLATION FROM NARROW TEMPERATURE INTERVALS.
- ESTABLISH AND UNDERSTAND THE KINETICS OF B AND Al SPECIES COMBUSTION REACTIONS IMPORTANT TO ADVANCED PROPULSION SYSTEMS.

TECHNIQUE

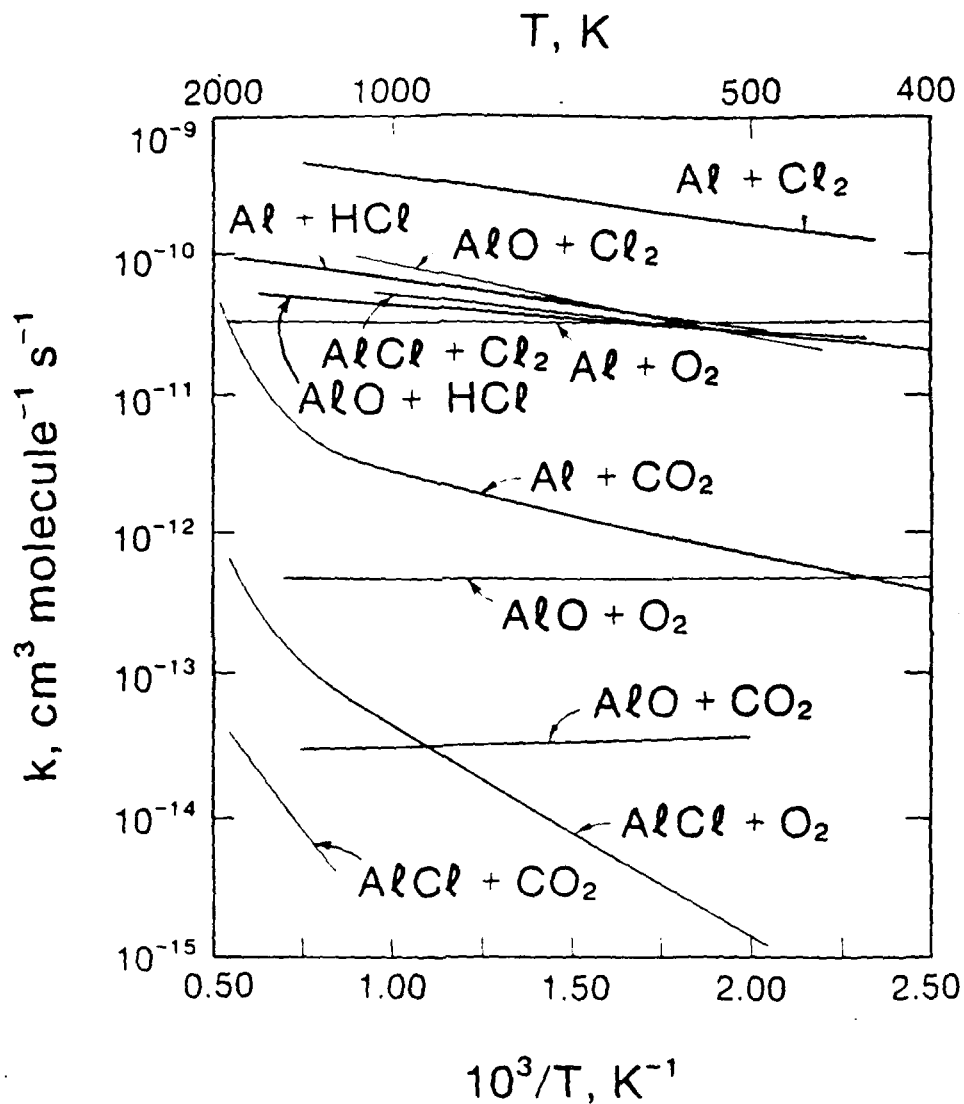
- HIGH TEMPERATURE FAST-FLOW REACTOR WITH LASER-INDUCED FLUORESCENCE AND MASS SPECTROMETRIC DETECTION.



- RESULTS OBTAINED THUS FAR HAVE ESTABLISHED THE RELIABILITY OF THE HTFFR TECHNIQUE.

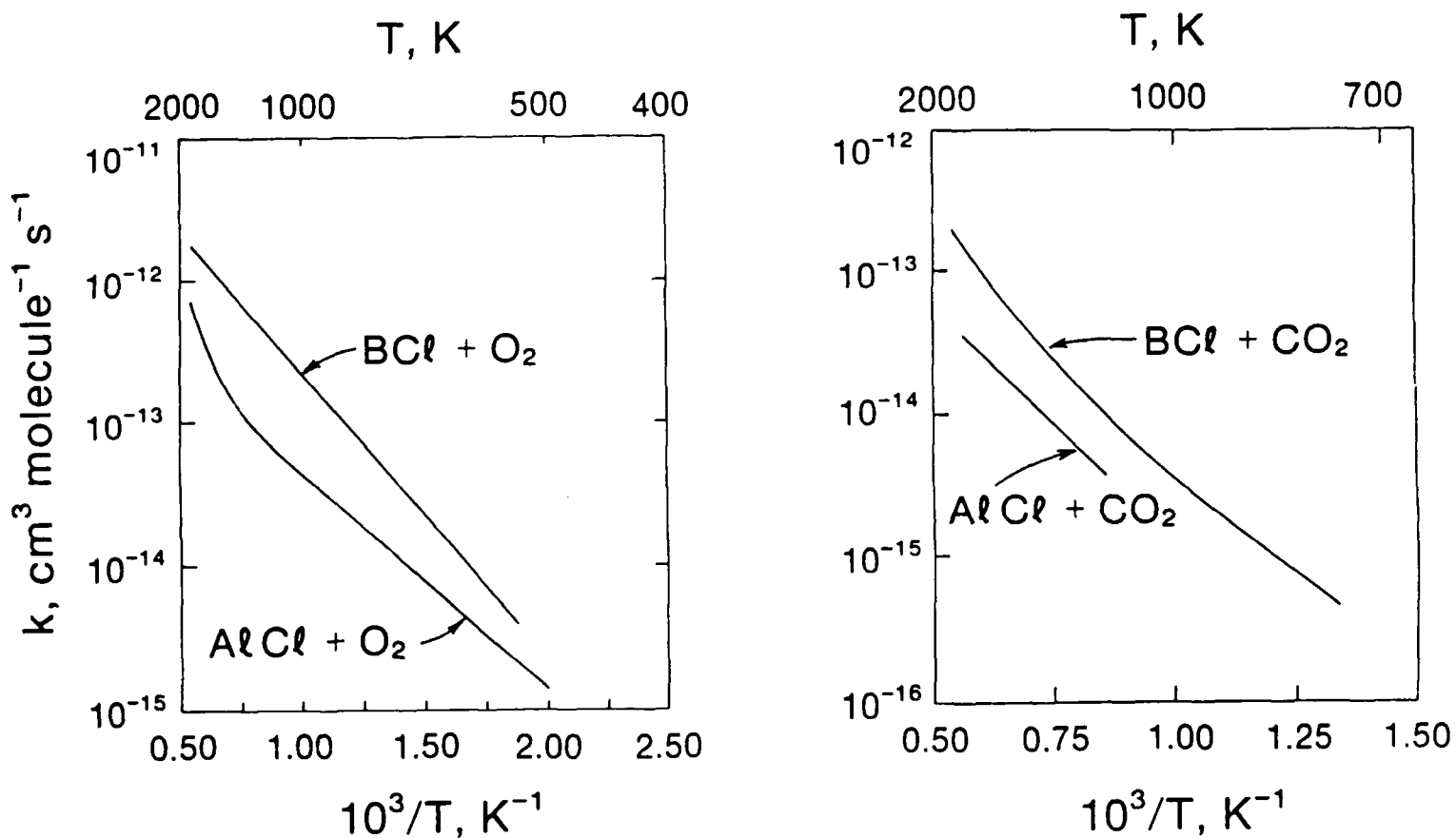
Figure 2

AIR FORCE BASIC RESEARCH ACHIEVEMENT



- EXTENSIVE SET OF Al-DATA NOW PREPARED FOR USE IN DEVELOPMENT OF ADVANCED SYSTEMS.
- ESTABLISHED THAT CURRENT CHEMICAL KINETIC THEORIES ARE INADEQUATE FOR PREDICTIONS ON Al REACTIONS.

Figure 3
**AIR FORCE BASIC RESEARCH
 ACHIEVEMENT**



- **MEASUREMENTS ON B-SPECIES HAVE BEGUN. ALLOW COMPARISON TO Al-SPECIES REACTIONS.**

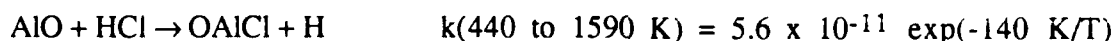
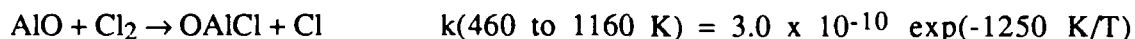
3. D.F. Rogowski and A. Fontijn, "The Radiative Lifetime of AlCl A¹I¹", *Chemical Physics Letters*, 137, 219-222 (1987).
4. A.G. Slavejkov, D.F. Rogowski and A. Fontijn, "An HTFFR Kinetics Study of the Reaction Between BCl and O₂ from 540 to 1670 K", *Chemical Physics Letters*, 143, 26-30 (1988).
5. D.F. Rogowski, P. Marshall and A. Fontijn, "High-Temperature Fast-Flow Reactor (HTFFR) Kinetics Studies of the Reactions of Al with Cl₂, Al with HCl and AlCl with Cl₂ Over Wide Temperature Ranges", *The Journal of Physical Chemistry*, in press.

These publications are appended to this final report.

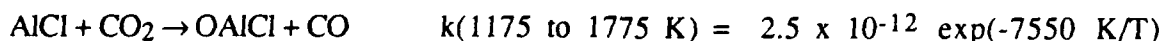
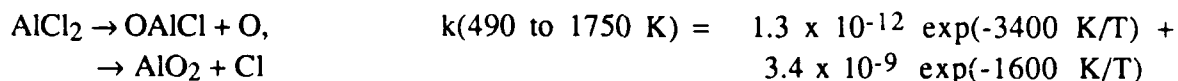
B. Partially Completed Studies

1. A.G. Slavejkov, C.T. Stanton and A. Fontijn, "High-Temperature Fast-Flow Reactor (HTFFR) Kinetics Studies of the Reactions of AlO with Cl₂ and HCl Over Wide Temperature Ranges, *The Journal of Physical Chemistry*, in preparation.

The studies of these two reactions complete those of the k(T) for the Al/O/Cl reaction system, compare Fig. 2. The following results were obtained (all rate coefficients given in this report are in cm³ molecule⁻¹ s⁻¹ units):



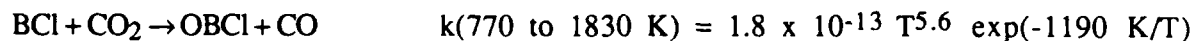
The rather small activation energy for the Cl₂ reaction and the near-negligible activation energy for the HCl reaction offer an interesting contrast to the OAlCl formation reactions from AlCl. There we obtained (see Appendices 1 and 2):



Apparently a large barrier exists in the formation of OAlCl coming from the AlCl-side, but not from the AlO-side. The reason for this is likely to be that AlO has an unpaired electron in its doublet ground state, whereas AlCl is a singlet species, which has to undergo a spin flip during reaction. Finally, it should be remarked that since OAlCl is not a radical, but an (unstable) molecule with no free valences, it is likely to be a bottleneck in the complete combustion of Al in perchlorate propellants, similar to the role of HOBO in boron combustion.

2. BCl/CO₂ Manuscript not yet begun.

The following result was obtained:



This is the first reaction involving a B or Al species, in which there is on thermochemical grounds only one possible product channel, for which the type of curvature in Arrhenius plots normally seen in hydrocarbon oxidation reactions, has been observed. That type of curvature is best described by a three-parameter fit expression of the form $k(T) = aT^b \exp(-c/T)$, as given here. However, the value of $b = 5.6$ is larger than simple transition state theory (TST) would predict. The fact that chemically B is more a metalloid than a metal (notwithstanding its potential use as a "metal" in metallized propellants), may bear on this behavioral similarity to hydrocarbon reactions. However, this result, also has a possible parallel to our findings for the AlCl + O₂ reaction (Appendix 1). There we found that $k(T)$ could be expressed equally well by the double-exponential expression, given above, as by $k(T) = 5.6 \times 10^{-28} T^{4.57} \exp(308 \text{ K}/T)$. As that reaction has two thermochemically accessible product channels, and the $b = 4.57$ value is again a high one, we favored the two-channel double exponential explanation. However, the BCl + CO₂ result makes the single channel three-parameter interpretation more probable than before. The mass spectrometric

product analysis of the $\text{AlCl} + \text{O}_2$ reaction will have to decide between the two possibilities.

C Some General Observations

The work of Fig. 3 is expected to be the beginning of an extensive comparison between B and Al species reactions. The differences in curvature in the Arrhenius plots and the magnitude of the rate coefficients suggest that it would be imprudent to make quantitative predictions from one set of reactions to the other, notwithstanding the position of B and Al in the same column of the periodic table. Ultimately a B-equivalent of the Al-reaction set shown in Fig. 2 should be prepared.

As a practical point it may be noted from Fig. 3 that the $\text{BCl} + \text{O}_2$ reaction is, in the temperature region observed, significantly faster than the $\text{AlCl} + \text{O}_2$ reaction. However if the trends continue the AlCl reaction should be faster above 2300 K. This is in contrast to the CO_2 reactions where the present data and the extrapolations of the $k(T)$ expressions indicate the BCl reaction to be faster at all temperatures.

In the course of this work several attempts have been made to use existing theories to try to fit our data, most extensively this has been done in Appendix 5, for the $\text{Al} + \text{Cl}_2$, $\text{Al} + \text{HCl}$ and $\text{AlCl} + \text{Cl}_2$ reactions, and in the paper in progress on the AlO reactions with Cl_2 and HCl. We found TST no help in predicting or describing the trends. While an electron jump mechanism gave good agreement with the data at midrange for the $\text{Al} + \text{Cl}_2$ and $\text{AlO} + \text{Cl}_2$ reactions (the latter may be fortuitous), it cannot predict temperature dependences. To obtain better predictive abilities, theory will have to be developed. We are trying to interest theoreticians in doing so. For Al reactions we have now provided a data base for them to use. Finally, molecular beam studies of the reaction dynamics should usefully complement our efforts. The group of Dorthe, Costes and Naulin at

Bordeaux have made a beginning with this.** Dr. Fontijn just finished a three-month visit to their laboratory, during which plans for future coordination of work were made.

III. PROFESSIONAL PERSONNEL

Donald F. Rogowski and Alexander G. Slavejkov performed the experimental work discussed in Section II. The former, in February 1988, successfully defended his Ph.D. thesis entitled "Gas-Phase Kinetics Studies of Reactions of Al, AlCl, and AlO with Cl₂, HCl, O₂ and CO₂ in a High-Temperature Fast-Flow Reactor" based on the AFOSR work. Mr. Slavejkov's Ph.D. is scheduled for 1990. Dr. Paul Marshall and Dr. Clyde T. Stanton, postdoctoral fellows, have participated in the theoretical interpretation of the results. The latter, whose salary has been funded entirely by NRL/ONR under a training arrangement, has spent most of the final nine months of the grant working on getting the mass-spectrometer HTFFR system operational, a process nearing completion. This system was largely constructed earlier in the grant period by David A. Stachelczyk and William F. Flaherty, who is continuing work with it.

IV. PRESENTATIONS AND OTHER INTERACTIONS

We presented papers and seminars in which results of our AFOSR-sponsored work were discussed, at the:

1. Department of Chemistry, University of Toronto, Toronto, Ont. (May 1986).
2. McDonnell Douglas Research Laboratories, St. Louis, MO (May 1986).
3. AFOSR/ONR Contractors Meeting on Combustion, Stanford University, Stanford, CA (June 1986).

M. Costes, C. Naulin, G. Dorthe, C. Vaucamps and G. Nouchi, "Dynamics of the Reactions of Aluminium Atoms Studied with Pulsed Crossed Supersonic Molecular Beams", *Faraday Discuss. Chem. Soc.*, **84, 75 (1987).

4. Twenty-First International Symposium on Combustion, Munich, W. Germany (August 1986).
5. Departments of Chemical Physics and Chemical Kinetics, S.R.I. International, Menlo Park, CA (October, 1986).
6. Department of Applied Mechanics and Engineering Sciences, University of California at San Diego, La Jolla, CA (October 1986).
7. Army Ballistic Research Laboratory, Aberdeen Proving Ground, MD (May 1987).
8. Naval Research Laboratory, Washington, DC (May 1987).
9. AFOSR/ONR Contractors Meeting on Combustion and Rocket Propulsion, Pennsylvania State University, University Park, PA (June 1987).
10. Eighteenth Symposium on Free Radicals, Oxford, England (September 1987).
11. Chemical Thermodynamics Division, National Bureau of Standards, Gaithersburg, MD (November 1987).
12. American Institute of Chemical Engineers, Annual Meeting, New York City, NY (November 1987).
13. Departments of Chemistry and Chemical Engineering, Illinois Institute of Technology, Chicago, IL (March 1988).
14. Chemistry Division, Argonne National Laboratory, Argonne, IL (March 1988).
15. School of Mechanical Engineering, Purdue University, West Lafayette, IN (March 1988).
16. Department of Chemistry, University of Denver, Denver, CO (March 1988).
17. JANNAF Panel Meeting on Kinetic and Related Aspects of Propellant Combustion Chemistry, Applied Physics Laboratory, John Hopkins University, Silver Springs, MD (May 1988).
18. AFOSR/ONR Contractors Meeting on Combustion, Rocket Propulsion and Diagnostics of Reacting Flows, California Institute of Technology, Pasadena, CA, June 1988.
19. American Chemical Society Symposium on Colloid and Surface Science, Pennsylvania State University, University Park, PA (June 1988).

20. Tenth International Symposium on Gas Kinetics, University College, Swansea, Wales (July 1988).
21. Department of Physics, University of Nijmegen, Nijmegen, The Netherlands (September 1988).
22. Department of Physical Chemistry, University of Bordeaux, Talence, France (October 1988).
23. Department of Chemistry, University of Leuven, Leuven, Belgium (November 1988).
24. American Institute of Chemical Engineers, Annual Meeting, Washington, D.C. (November 1988).

Dr. C.W. Larson of the Air Force Astronautics Laboratory, and other Air Force Personnel, contacted us several times in 1986 and 1987 to discuss the design of a high-temperature reactor for use in spectroscopic measurements on hydrogen/metal-vapor mixtures. They are interested in such information in the context of the Solar Plasma Propulsion Program. We maintain frequent contacts with Drs. D.P. Weaver, and T. Edwards of that laboratory. In the last year this has led to discussions about the potential means for those investigators to study metal-oxidation reactions above 2000 K, i.e., above our current high-temperature limit. Dr. J. Lurie, of Aerodyne Research Inc., called us to obtain information on our AlCl radiative lifetime measurements for their plume model calculations for AEDC. The results (Appendix 3) have already been incorporated in their rocket plume uv band model calculations. Dr. M.W. Chase of the National Bureau of Standards had several conversations with us on the implications of our measurements for entries on aluminum species in the JANAF Thermochemical Tables. We have initiated some collaboration with Dr. J.R. McDonald's group at N.R.L., in connection with their BH-compound combustion research and our mass spectrometric work. I (A.F.) have served as a member of the ONR Board of Visitors for review of their Mechanics Division Program. Dr. J. Eversole of N.R.L. called to discuss surface reactions of

levitated boron particles. Dr. B.N. Ganuly of AFAWL/POOC expressed an interest in our results for the development of better flares and made some preliminary inquiries about obtaining an HTFFR for their work on that problem. Dr. J.F. Paulson of the Air Force Geophysics Laboratory visited with several of his collaborators to look at our high-temperature technology, which they want to apply to ion reactions of importance to the National Aerospace Plane. In addition to the meetings mentioned above, Dr. Fontijn also had many discussions with Air Force Personnel and contractors at the June 1987 EMHIAT and the March 1988 AFOSR Combustion Instability Workshops.

AN HTFFR KINETICS STUDY OF THE REACTION BETWEEN AlCl and O_2 FROM 490 TO 1750 K.

DONALD F. ROGOWSKI AND ARTHUR FONTIJN

Department of Chemical Engineering
Rensselaer Polytechnic Institute,
Troy, NY 12180-3590

A method for the production of AlCl radicals in an HTFFR (high-temperature fast-flow reactor) is described. Their relative concentration in the title reaction is monitored by laser-induced fluorescence. The overall reaction rate coefficients, for AlCl consumption by O_2 , can be fitted by the expression $k(T) = 1.3 \times 10^{-11} \exp(-3400\text{K}/T) + 3.4 \times 10^{-12} \exp(-16100\text{K}/T)$ $\text{cm}^3 \text{molecule}^{-1} \text{s}^{-1}$. Error limits are discussed in the text. The results are shown to be compatible with a mechanism where the $\text{AlO}_2 + \text{Cl}$ product channel dominates at lower temperatures, while the $\text{OAlCl} + \text{O}$ channel dominates at higher temperatures. The $\ln k(T)$ versus T^{-1} dependence of the $\text{AlCl} + \text{O}_2$ reaction is contrasted to those observed for the $\text{AlO} + \text{O}_2$ and $\text{BF} + \text{O}_2$ reactions.

Introduction

The development and use of the HTFFR technique¹ is leading to an experimental data base of homogeneous gas-phase oxidation reactions of metallic species. Measurements of rate coefficients $k(T)$ in the 300–1900 K range have been reported and the results have been summarized in several reviews.^{2–4} A variety of $k(T)$ dependences have been observed, including normal Arrhenius $k(T) = A \exp(-E_a/RT)$ behavior, temperature independent rate coefficients and reactions with a slight negative activation energy. In addition, reactions have been found the rates of which are determined primarily by the thermal equilibrium populations of excited states of the reactants. While the original studies were concerned with reactions of metal atoms, we now concentrate on reactions of metallic radicals. Here we report on the first HTFFR study of an oxidation reaction of a monohalide radical, AlCl .

2. Technique

2.1. Reactor and Reactants

Basic HTFFR designs have been discussed previously.⁵ The present reactor is shown schematically in Fig. 1. A vertical ceramic reaction tube is surrounded by resistance heating elements and insulation inside a vacuum can. At the upstream (lower) side the gaseous metallic reactant is produced and entrained in Ar bath gas. A movable inlet system allows for introduction of the oxidant from 20 to 0 cm upstream of

the observation plane, where the relative concentration of the metallic species is measured by laser-induced fluorescence (LIF). A reactor with silicon carbide rod heating elements, described recently,⁵ had to be modified due to its exposure to chlorine in the present experiments. A mullite (McDaniel MV 30) 2.2 cm i.d. reaction tube was employed, which contrary to the 998 grade alumina used in earlier HTFFR work, is resistant to chlorine at elevated temperatures. The other change concerns the oxidant inlet system, which used to consist of 998 alumina tube tipped by a multihole Pt ring. As Pt too is not resistant to chlorine at high temperatures, mullite was used for the entire O_2 inlet system. The vertical 0.3 cm o.d. inlet tube was fitted with a 0.6 cm o.d., 1.5 cm long horizontal tube with two 0.1 cm holes for the O_2 introduction.

Initial experiments on the production of AlCl led to development of the following method. A trace of Cl_2 , typically < 0.005% of the Ar flow, was added to the Ar bath gas and passed over a tungsten coil wetted with Al. At temperatures below 1000 K it was necessary to heat the coil by passing a current through it to obtain usable intensities of AlCl fluorescence, F_{AlCl} . Above that temperature no current was applied and the coil was withdrawn to a cooler zone of the reaction tube, otherwise F_{AlCl} too large for convenient measurements were produced. The flow of Cl_2 was adjusted to maximize the AlCl fluorescence signal. At high average gas velocities, addition of small quantities of O_2 resulted in a sharp decrease in F_{AlCl} . This

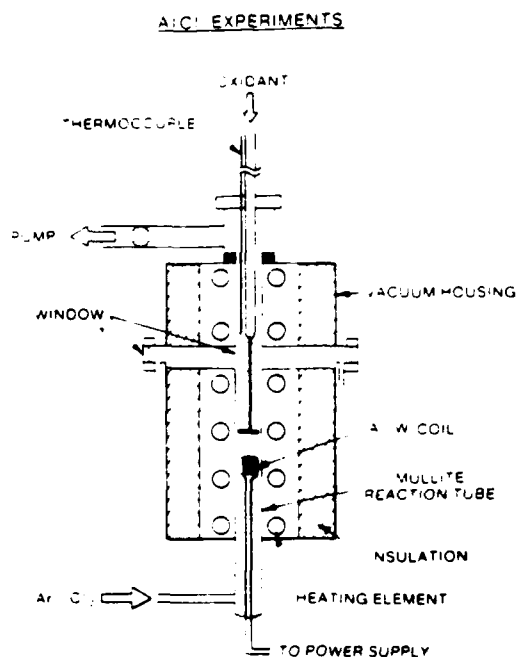


FIG. 1. Schematic of the HTFFR used.

decrease was followed by a more gradual decrease with increasing $[O_2]$, which was comparable to that observed at low flow velocities. The sharp decrease can be attributed to removal of free Al atoms by the fast Al/O_2 reaction,⁶ which terminates the AlCl production. The lowest $[O_2]$ used in the AlCl/ O_2 rate coefficient measurements always exceeded that required to terminate AlCl production. These observations show that the AlCl production occurred at least partially in the gas phase rather than on the coil. The necessity of suppressing AlCl production downstream of the inlet by addition of an initial O_2 flow made it impossible to obtain traversing inlet mode data^{1,3,6} with the present design. Instead, stationary inlet measurements³ at different inlet positions were made.

A small quantity of Ar (about 2% of the bath gas flow) was introduced through the oxidant inlet to improve the response time for the stabilization of the AlCl signal after a change in O_2 flow. The gases used, obtained from Linde, were 99.5% Cl_2 , 99.998% Ar (from liquid Ar) and 99.6% O_2 . In a few preliminary experiments 99.995% O_2 was used, yielding no difference in the observations.

2.2. Measurements and Data Reduction

For the LIF measurements a Lambda Physik EMG 101 excimer FL 2002 dye laser was used. Coumarin 334 dye was used to produce 522.8

nm radiation, which was frequency doubled with a KDP crystal to pump the AlCl A-X(0,0) transition at 261.4 nm. Fluorescence at the same wavelength was observed through a 262 ± 13 nm (FWHM) interference filter. The detection system consisted of an EMI 9813QA photomultiplier tube operated from 1300 to 1600 V. The PMT output was recorded with a Data Precision Analogic 6000 620 100 MHz transient digitizer. The averages of 100 pulses were used for the fluorescence intensity measurements to smooth out the variations in the laser pulse energy. The presence of a side tube from the reaction tube to the fluorescence observation window reduced the laser background signal typically to less than 10% of the fluorescence signal at the minimum $[O_2]$. F_{AlCl} . Rate coefficients were measured at O_2 inlet to observation plane distances of 10 cm and 20 cm, following the procedures described previously.^{3,3} Plots of $\ln [AlCl]_{rel} = \ln (F_{AlCl}/F_{AlCl})$ versus $[O_2]$ yielded straight lines with slopes kt , where t is the reaction time. During these experiments pressure was measured downstream of the reaction zone with an MKS Baratron gauge. To determine the reaction temperature, an unshielded type R thermocouple was traversed through the reaction zone immediately after a run. After all the experiments had been completed pressure corrections, and temperature corrections, from a shielded thermocouple, were obtained following the recommendations of Fontijn and Felder.^{3,7}

A weighted linear regression and full propagation of errors treatment, as described by Fontijn and Felder,³ was used to determine the uncertainty in kt and in turn k for the particular temperature T , pressure P and average gas velocity \bar{v} used. In the treatment, uncertainty in both $[AlCl]_{rel}$ and $[O_2]$ are taken into account by combining them vectorially, to obtain the error in kt . The regression of k as a function of temperature, with errors in both k and T was obtained by minimizing $\chi^2 = \sum w_i^2 (\ln k_i - \ln \hat{k}_i)^2$ where \hat{k}_i is the fitted and k_i the experimental value. The weighting factor, w_i^2 , accounts for errors in both k and T by combining them vectorially, $w_i^{-2} = \sigma_{k,i}^{-2} + [d(\ln k_i)/dT]^2 \sigma_{T,i}^2$.

3. Results

Measurements of the rate coefficients for AlCl consumption by O_2 were made from 400 to 1750 K, spanning a range of k values from about 1×10^{-13} to 1×10^{-12} cm³ molecule⁻¹ s⁻¹. Ninety-one measurements were taken and the eighty-six with correlations $r \geq 0.95$ for regressions of $\ln [AlCl]_{rel}$ vs. $[O_2]$ were accepted. In

previous work³ drift in the Al flux from the coil was encountered. In this work this resulted in a drift in F_{AlCl} . A measure of the variation is the difference of F_{AlCl} at the beginning and end of a k measurement divided by their average. All of the eighty-six data points used showed this variation to be less than ± 0.50 . For seventy-five of the measurements, the variation was less than ± 0.25 .

The measurements are summarized in Table I. Inspection of the data shows the k values to be independent of the implicit parameters: inlet position, \bar{P} , $[M]$ (average total concentration), F_{AlCl} (and hence $[\text{AlCl}]_{\text{inlet}}$) and \bar{v} . The results are also independent of the $[\text{Cl}_2]$ added, which were in the range 4×10^{12} to 1×10^{14} cm⁻³ depending on the $[\text{Ar}]$ used. Temperatures given are averages of the values from measurements at 5 cm intervals from the observation zone to the O₂ inlet position, corrected as discussed above. The standard deviation about the mean gas temperature varied from ± 1 to ± 30 K depending on the reaction conditions.

The independence of k with respect to inlet position and reaction time indicates that any quenching of AlCl (A) by O₂ does not affect the k measurements. We have observed the radiative lifetime of AlCl to be $\approx 10^{-8}$ s, yielding $k_{\text{rad}} \approx 10^8$ s⁻¹. Assuming a maximum value for the rate coefficient for quenching by O₂, $k_q \approx 10^{-10}$ cm³ molecule⁻¹ s⁻¹ and using the maximum $[\text{O}_2]$ used of 10^{16} cm⁻³, $k_{\text{rad}}/k_q[\text{O}_2] \approx 10^2$, showing that quenching by O₂ is insignificant.

Various fits of the k data versus T^{-1} were made. A good fit was obtained to a double exponential $k(T) = A \exp(-B/T) + C \exp(-D/T)$ expression. Analysis for this fit results in:

$$k(T) = 1.26 \times 10^{-12} \exp(-3400K/T) + 3.36 \times 10^{-9} \exp(-16100K/T) \text{ cm}^3 \text{ molecule}^{-1} \text{ s}^{-1} \quad (1)$$

To calculate the statistical uncertainty in k both the variances associated with each parameter and the covariances associated with the different pairs of parameters must be taken into account, since the parameters are not independent.⁴ The variances and covariances associated with Eq. (1) are $\sigma_A^2 = 5.622 \times 10^{-26}$; $\sigma_{AB} = 3.908 \times 10^{-11}$; $\sigma_{AC} = 3.433 \times 10^{-22}$; $\sigma_{AD} = 2.051 \times 10^{-10}$; $\sigma_B^2 = 2.864 \times 10^{-4}$; $\sigma_{BC} = 2.044 \times 10^{-7}$; $\sigma_{BD} = 1.238 \times 10^3$; $\sigma_C^2 = 1.161 \times 10^{-17}$; $\sigma_{CD} = 5.871 \times 10^{-7}$; $\sigma_D^2 = 3.023 \times 10^6$. From these σ_k was calculated in the standard manner,⁹ with a 10% added systematic uncertainty in the flow profile factor.³ The $2\sigma_k$ confidence levels are shown in Fig. 2. These

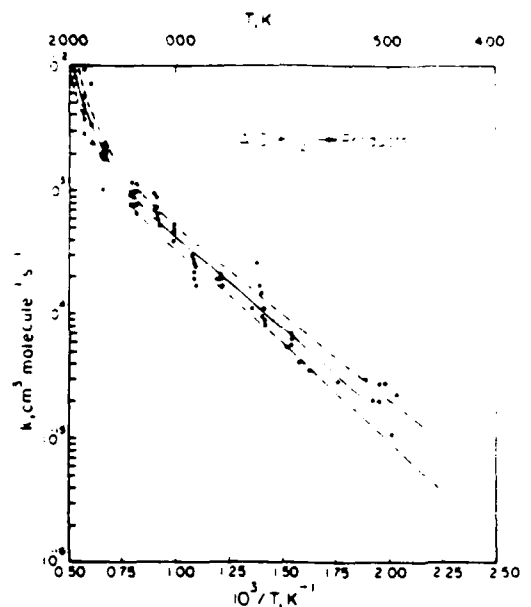


FIG. 2. Rate coefficient data for the AlClO₂ reaction

— Double exponential rate expression fit of data given in text.
 - - - Two standard deviations to the fit of the rate expression as described in the text.

levels vary somewhat over the temperature range investigated and are $\pm 19\%$ at 500, $\pm 12\%$ at 700, $\pm 11\%$ at 1000 and $\pm 14\%$ at 1800 K. It should be noted that σ_k represents the standard deviation of the fitted expression, not the standard deviation of the measurements of k .

A good transition state fit, $k(T) = E/T^2 \exp(-G/T)$, was also obtained.

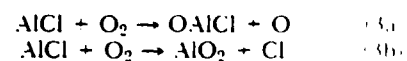
This fit yields

$$k(T) = 5.62 \times 10^{-28} T^{4.77} \exp(308 K/T) \text{ cm}^3 \text{ molecule}^{-1} \text{ s}^{-1} \quad (2)$$

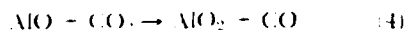
$2\sigma_k$ confidence levels shown in Fig. 3 were calculated similarly to those for Eq. (1). The variances and covariances associated with Eq. (2) are $\sigma_E^2 = 6.039 \times 10^{-54}$; $\sigma_{EF} = -1.353 \times 10^{-27}$; $\sigma_{EG} = 1.306 \times 10^{-24}$; $\sigma_F^2 = 3.034 \times 10^{-10}$; $\sigma_{FG} = -2.917 \times 10^2$; $\sigma_G^2 = 2.904 \times 10^3$. The $2\sigma_k$ confidence levels derived from these are $\pm 19\%$ at 500, $\pm 11\%$ at 700, $\pm 11\%$ at 1000 and $\pm 12\%$ at 1800 K.

4. Discussion

The following reaction pathways have to be considered



Both are allowed by the spin-conservation rule. Based on current JANAF ΔH_{298}° values the abstraction reaction (3a) is 47 kJ mole^{-1} exothermic, while the substitution reaction (3b) would be 87 kJ mole^{-1} endothermic.¹⁰ The latter value would lead to minimum activation energies too large to allow the observed rate coefficients. However, our observation that the reaction



has a slight negative activation energy indicates that the new O-Al bond in O-Al-O is at least equal to the strength of the O-CO bond, resulting in an $\Delta H_{298}^{\circ} \text{AlO}_2 \leq -199 \text{ kJ mole}^{-1}$. This is 113 kJ mole^{-1} more exothermic than the current JANAF value, which is based on mass spectrometry evaporation experiments.¹¹ Possibly, different AlO_2 structure may be responsible for this difference. It should be noted that other mass spectrometry evaporation studies¹² suggest a heat of formation which is more in agreement with that from our³ work. On this³ revised basis reaction (3b) has a $\Delta H_{298}^{\circ} \leq -26 \text{ kJ mole}^{-1}$, i.e. is also exothermic. Thus on thermochemical grounds (3b) now has to be considered a possible path for the AlCl/O_2

reaction. In fact, if the double exponential Eq. (1) correctly describes the kinetics, (3b) may be identified with the first term which dominates at the lower temperatures. An A factor of $1 \times 10^{12} \text{ cm}^3 \text{ molecule}^{-1} \text{ s}^{-1}$ would be small for the simple abstraction reaction (3a). The second term of Eq. (1), which is significant at high temperatures, has a large pre-exponential indicative of an abstraction reaction such as (3a). While a value of $3.4 \times 10^{11} \text{ cm}^3 \text{ molecule}^{-1} \text{ s}^{-1}$ does not appear physically reasonable, it has a large uncertainty σ , associated with it. Clearly this pre-exponential must be larger than that of the first term to account for the observed increase in slope. As can be seen this increase occurs near the upper temperature limit investigated. An extension to much higher temperatures than accessible by our apparatus would be required to determine this term more accurately, though k near the upper limit of the current temperature range is well known, as noted above.

While the two-path model for reaction (3) thus appears quite reasonable, the equally good fit of the data to the transition state type expression (2) indicates that it merits further discussion. However, the magnitude of the power of T , 4.57, does appear unusually high for a reaction of small molecules,^{2,13,14} and contrary to the term just discussed for Eq. (1), it has a small associated uncertainty σ_B . We therefore favor Eq. (1), although experimental product identification is needed. Unfortunately neither OAlCl nor AlO_2 have known electronic transition spectra, which precludes the use of the present diagnostic LIF to settle this problem. Mass spectrometer HTFR experiments which should allow product identification are planned; the apparatus is being constructed.

The $\ln k(T)$ versus T^{-1} dependence of the AlCl/O_2 reaction, Figs. 2 and 3, contrasts sharply with that of its O-atom equivalent



which, like reaction (4), has a slight negative activation energy.³ That behavior is indicative of the formation of an intermediate reaction complex, such as O-O-Al-O, which preferentially dissociates to the original reactants rather than products.^{2,4,5} The temperature dependence of reaction (3) indicates that when the O atom in AlO is replaced by a Cl atom, either no such complex is formed or that it dissociates preferentially to products. This is similar to the suggested behavior of the reaction¹⁵

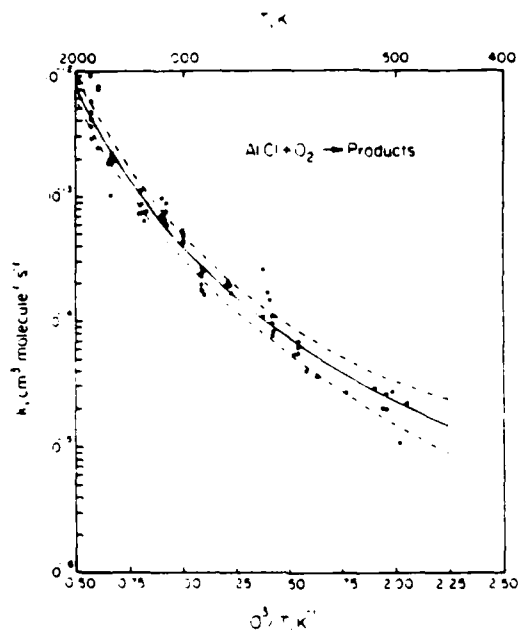


FIG. 3. Rate coefficient data for the AlCl/O_2 reaction. — Transition-state type rate expression fit of data given in text. --- Two standard deviations to the fit of the rate expression as described in the text.

AlCl radical reactions may be expected to show some similarity to those of the BF radical, which is constituted of the elements above Al and Cl, respectively, in the periodic table. For the reaction between BF and O₂, $k(T)$ has been reported¹⁹ to be $1.8 \times 10^{11} \exp(-7240K/T)$ cm³ molecule⁻¹ s⁻¹ from 675 to 1030 K. In that work no curvature in the Arrhenius plot was observed and an OBF = O product was assumed. However, the limited temperature range investigated would make it difficult to establish curvature and competition from a BO₂ product channel, the equivalent of the products of reaction (3b), has to be considered. Both BF/O₂ product channels would also be exothermic.

Acknowledgement

We thank Dr. Paul Marshall for helpful discussions. This work was supported under Grants AFOSR-82-0073 and 86-0019. The United States Government is authorized to reproduce and distribute reprints for governmental purposes notwithstanding any copyright notation thereon.

REFERENCES

1. FONTIJN, A., KURZIUS, S. C., AND HOUGHTON, J. J.: *Fourteenth Symposium (International) on Combustion*, p. 167. The Combustion Institute, 1973.
2. FONTIJN, A. AND ZELLNER, R.: *Reactions of Small*

- Transient Species, Kinetics and Energetics* (A. Fontijn and M.A.A. Clyne, Eds.), Chap. 1, Academic Press, 1983.
3. FONTIJN, A. AND FELDER, W.: *Reactive Intermediates in the Gas Phase: Generation and Monitoring* (D.W. Setser, Ed.), Chap. 2, Academic Press, 1979.
 4. FONTIJN, A.: *Combust. Sci. Technol.* **5**, 171 (1986).
 5. ROGOWSKI, D.F., ENGLISH, A.J. AND FOSTER, A.J.: *J. Phys. Chem.* **90**, 1688 (1986).
 6. FONTIJN, A., FELDER, W. AND HOUGHTON, J.J.: *Sixteenth Symposium (International) on Combustion*, p. 871. The Combustion Institute, 1977.
 7. FONTIJN, A. AND FELDER, W.: *J. Phys. Chem.* **83**, 24 (1979).
 8. BEVINGTON, P.R.: *Data Reduction and Error Analysis for the Physical Sciences*, McGraw-Hill, 1969.
 9. WENTWORTH, W.E.: *J. Chem. Ed.*, **42**, 96 (1965).
 10. JANAF Thermochemical Tables, Data sheets available in 1985. Dow Chemical Co.
 11. HO, P. AND BURRS, R.P.: *High Temp. Sci.* **12**, 31 (1980).
 12. SRIVASTAVA, R.D., AND FARBER, M.: *Proc. Indian Acad. Sci. (Chem. Sci.)* **90**, 257 (1981).
 13. WARNATZ, J.: *Combustion Chemistry* (W.C. Gardiner, Jr., Ed.), Chap. 3, Springer, New York, 1984.
 14. HANSON, R.K. AND SALIMIAN, S.: *ibid.*, Chap. 9.
 15. LLEWELLYN, I.P., FONTIJN, A. AND CLYNE, M.A.A.: *Chem. Phys. Lett.* **84**, 504 (1981).
 16. LIGHT, G.C., HERM, R.R. AND MATSUMOTO, J.H.: *J. Phys. Chem.* **89**, 3066 (1985).

COMMENTS

Jay B. Jeffries, SRI, Int. Menlo Park, CA 94301 USA.
What diagnostics have been performed to determine the rate of wall loss of the Al, AlCl, AlO compounds on the hot mullite walls of your reactor? Do you expect the probable fast rate to impact your reported data?

Author's Reply. The fact that wall losses can indeed be fast was established in several of the earliest HTFFR studies² from plots of pseudo-first order rate coefficients versus oxidant concentrations. The wall-loss intercepts do not directly affect the obtained rate coefficients, which are derived from the slopes. It is likely that variation in wall losses over the period of the measurement of one rate coefficient is partially responsible for the scatter in the data. Early work showed the scatter to be considerably stronger in N₂ than Ar, which observation points in that direction. Hence, Ar is now used as bath gas. The whole subject of accuracy in HTFFR rate coefficient measurements has been discussed extensively in Refs. 3 and 4.

REFERENCES

1. FONTIJN, A., KURZIUS, S. C. AND HOUGHTON, J. J.: *Fourteenth Symposium (International) on Combustion*, p. 167. The Combustion Institute, 1973.
2. FONTIJN, A., FELDER, W. AND HOUGHTON, J. J.: *Fifteenth Symposium (International) on Combustion*, p. 775. The Combustion Institute, 1975.
3. FONTIJN, A. AND FELDER, W.: *J. Phys. Chem.* **83**, 24 (1979).
4. FONTIJN, A. AND FELDER, W.: *Reactive Intermediates in the Gas Phase: Generation and Monitoring* (D.W. Setser, Ed.), Chap. 2, Academic Press, 1979.

Stephen L. Baughcum, Los Alamos Nat. Lab., Los Alamos, N.M. 87545 USA. Aluminum chloride exists in both the monovalent (AlCl) and trivalent (AlCl₃) forms, which probably have different reactivities with oxygen and different sticking coefficients upon wall collisions. Clearly the amount of AlCl relative to AlCl₃

will be sensitive to the Cl_2 pressure in the system. In your experiments, how much AlCl_3 is produced relative to AlCl and could secondary production of AlCl via equilibration from AlCl_3 affect the results?

Author's Reply. Generation of AlCl from AlCl_3 equilibration is not likely. AlCl is generated from Al and Cl_2 , so any AlCl_3 or AlCl_2 present must result from either a sequence of bimolecular reactions or from termolecular reactions. However, the reactions AlCl_2 and AlCl_2Cl have both been found to be independent of $[\text{M}]$, under our operating conditions and the Al reaction is much faster than the AlCl reaction. These points coupled with the 1×10^{-3} to 1×10^{-2} s residence times indicate that $[\text{AlCl}] \gg [\text{AlCl}_3]$ and $[\text{AlCl}_2]$. Calculations show that at equilibrium $[\text{AlCl}_3]$ and $[\text{AlCl}] \gg [\text{AlCl}_2]$, suggesting that in our experiments higher chlorides, if present, will not significantly react back to AlCl . Direct proof of the absence of significant secondary AlCl production comes from the observation that the rate coefficients in Table I are independent of reaction time, observation distance and flow velocity. Also, $[\text{Cl}_2]$ was varied by more than an order of magnitude without affecting k . Finally, since $[\text{O}_2]$ is much larger than the concentration of any other reactant, the $[\text{O}_2]$ is unaffected by any aluminum chloride reactions.

REFERENCES

1. ROGOWSKI, D. F. AND FONTIJN, A., work in progress.

Dr. Milton Farber, Space Sciences, Inc., 135 W. Maple Ave., Monrovia, CA 91016 USA. I would like to commend you on a very good set of experimental kinetics. The fact that your results are not compatible with the thermodynamic value for the ΔH_f of $\text{AlO}_2(\text{g})$ reported in 1980 by Ho and Burns,¹ but are quite compatible with our previously published values² can be readily explained. Your earlier papers on the kinetics of CO_2 and O_2 with AlO appeared to yield activation energies of approximately zero, also compatible with our value of -44 kcal/mole for ΔH_f of $\text{AlO}_2(\text{g})$, but incompatible with the value of -23.2 ± 6 kcal/mole reported by Ho and Burns.¹

First, I shall explain the reason for the incompatibility of your results with those of Ho and Burns. In 1976 and 1980 Burns and coworkers published two papers,^{1,3} one on the ΔH_f of $\text{Al}_2\text{O}_2(\text{g})$ and another on $\text{AlO}_2(\text{g})$. These were evaporation experiments in which he assumed "virtual equilibrium," with an accommodation coefficient of $\alpha = 0.325$ for the two species. These values are much too high for these species, by at least an order of magnitude for $\text{AlO}_2(\text{g})$. Nearly ten published papers have presented accommodation coefficients of less than 0.10 for the evaporation of $\text{Al}_2\text{O}_3(\text{g})$.⁴ Our experiments on the α of $\text{Al}_2\text{O}_3(\text{g})$ showed a result of approximately 0.08.⁵

The assumption by Ho and Burns¹ that the α for $\text{AlO}_2(\text{g})$ is 0.325 leads to a calculated partial pressure from the Langmuir expression, $p = n \sqrt{2\pi mkT} \alpha$, which is much too low, and results in a ΔH_f of $\text{AlO}_2(\text{g})$ some 20 kcal/mole too positive. His values for $\text{AlO}(\text{g})$ and $\text{Al}_2\text{O}(\text{g})$ are also too positive by 2 to 3 kcal/mole from the well established and universally recognized ΔH_f values for $\text{AlO}(\text{g})$ and $\text{Al}_2\text{O}(\text{g})$. His value for Al_2O_2 , a larger molecule with a much lower accommodation coefficient than 0.325 (the value also assumed by Fu and Burns¹), is some 15 kcal/mole more positive than the ΔH_f obtained from effusion equilibrium experiments. The high temperature mass spectrometer spark experiments on $\text{Al}_2\text{O}_3(\text{g})$ by Cornides and Gal⁶ show that initial decomposition species are atomic and that the atoms recombine to form the higher oxides. In general, evaporation decomposition experiments will not yield equilibrium pressures and thermodynamic data derived from them will be unreliable. One further comment: when I presented our data at the Faraday Symposium in London in 1973⁷ Professor Skinner remarked that the Al species with oxygen consisted of ionic bonding and that the Al-O bond strengths were nearly equal in all the species, AlOH , AlO , Al_2O , Al_2O_2 and AlO_2 , etc.

As noted, the compatibility between your results and ours can also be readily explained. Between 1970 and 1976 we published six papers on equilibrium studies leading to thermodynamic data for the aluminum oxide species.^{2,7,8-11} Four were performed in alumina effusion cells employing sapphire chips to ensure no interference with extraneous materials.^{2,8,10,11} Two mass spectrometer studies of Al additive compositions in H_2/O_2 flames confirmed the effusion studies.⁹ A $\Delta H_f^{\circ,298}$ of -44 ± 2 kcal/mole was obtained for $\text{AlO}_2(\text{g})$, the value with which your experiments agree. Prior to these studies a mass spectrometer investigation in 1960 by Drowart, et al¹² on the dissociation species over Al_2O_3 was performed employing tungsten and molybdenum cells. They reported thermodynamic data for $\text{AlO}(\text{g})$, $\text{Al}_2\text{O}(\text{g})$ and $\text{Al}_2\text{O}_2(\text{g})$ with values more positive than those obtained in our neutral cell effusion experiments and those of many other investigations for the heats of formation of $\text{AlO}(\text{g})$ and $\text{Al}_2\text{O}(\text{g})$. They did not observe $\text{AlO}_2(\text{g})$. Our calculations later showed that reactions took place between the metal cells and Al species,² resulting in more positive ΔH_f values and completely reducing the AlO_2 concentration to an undetectable level. If these reactions were taken into consideration the results of Drowart, et al¹² would be in good agreement with our data.

In conclusion, although the existence of $\text{AlO}_2(\text{g})$ and its heat of formation have been controversial for many years, I am pleased that your kinetic experiments are compatible with what I feel is a definitive value for the $\Delta H_f^{\circ,298}$ of $\text{AlO}_2(\text{g})$, -44 ± 2 kcal/mole. I look forward to the results of your forthcoming mass spectrometer experiments.

REFERENCES

1. HO, P. AND BURNS, R. F., High Temp. Sci. 12, 31 (1980).
2. FARBER, M., SRIVASTAVA, R. D., AND UY, O. M., J. Chem. Soc. Faraday I, 68, 249 (1972).
3. FU, C. M. AND BURNS, R. F., High Temp. Sci. 8, 353 (1976).
4. SRIVASTAVA, R. D. AND FARBER, M., Proc. Indian Acad. Sci. 90, 257 (1981).
5. FARBER, M. AND BUYERS, A. G., Proceedings of the Fifth Symposium on Thermophysical Properties, ASME, Newton, Mass., p. 483 (1970).
6. CORNIDES, I. AND GAL, T., High Temp. Sci. 10, 171 (1978).
7. FARBER, M., SRIVASTAVA, R. D., FRISCH, M. A. AND HARRIS, S. P., Faraday Symposium of the Chemical Society No. 8, p. 121 (1973).
8. FARBER, M., SRIVASTAVA, R. D. AND UY, O. M., J. Chem. Phys. 55, 4142 (1971).
9. FARBER, M. AND SRIVASTAVA, R. D., Combustion & Flame 27, 99 (1976).
10. SRIVASTAVA, R. D., UY, O. M. AND FARBER, M., J. Chem. Soc. Faraday II, 68, 1388 (1972).
11. FARBER, M. AND SRIVASTAVA, R. D., High Temp. Sci. 11, 1 (1979).
12. DROWART, J., DEMARIA, G., BURNS, R. P. AND INGHAM, M. G., J. Phys. Chem. 32, 1366 (1960).

Author's Reply. The greatest discrepancy between the $\Delta H_{f,298}^\circ$ values reported in the Kundsen cell evaporation literature and the limit value indicated by our kinetic studies is that encountered in our work on the reaction $\text{AlO} + \text{CO}_2 \rightarrow \text{AlO}_2 + \text{CO}$. There we observed a slightly negative activation energy, which indicates that the reaction cannot be endothermic. If we take current JANAF values for AlO , CO and CO_2 and the -29.6 kcal mole $^{-1}$ accuracy limit value from the Ho and Burns experiments and add your correction of about 20 kcal mole $^{-1}$, recommended above, reaction (1) would be approximately thermoneutral. Using the uncertainty limit value from your work it would still be some 4 kcal mole $^{-1}$ endothermic, possibly not very significant. The vexing question of the O-AlO bond energy may thus be resolved. Our planned mass spectrometer experiments will have to establish if no structural differences (e.g., OAlO vs. OOA) exist between AlO_2 from evaporation and kinetic studies.

REFERENCE

1. ROGOWSKI, D. F., ENGLISH, A. J. AND FONTIJN, A.: J. Phys. Chem. 90, 1688 (1986).

TABLE I
 Summary of Rate Coefficient Measurements of $\text{AlCl} + \text{O}_2 \rightarrow \text{Products}$

Oxidant Inlet Position (cm)	P (cm^2)	$[\text{M}]$ (cm^{-3})	$[\text{O}_2]$ Range (cm^{-3})	I_{exc}	v (ms $^{-1}$)	l (Å)	k ($\text{cm}^3 \text{ molecule}^{-1} \text{ s}^{-1}$)	σ
20	46.0	1.68(+17)	4.46(+14)	3.09(+15)	40	922	2.94(14)	3.48(15)
20	37.3	3.92(+17)	1.06(+15)	7.32(+15)	13	918	2.71(14)	1.63(15)
20	37.3	3.93(+17)	9.83(+14)	7.32(+15)	13	917	2.70(14)	1.32(15)
20	27.5	2.91(+17)	1.94(+14)	3.38(+15)	26	906	1.73(14)	1.30(15)
20	27.4	2.90(+17)	5.24(+14)	3.39(+15)	26	912	2.19(14)	2.29(15)
10	27.4	2.89(+17)	4.53(+14)	3.38(+15)	26	911	2.42(14)	2.30(15)
10	27.4	2.88(+17)	1.74(+14)	3.64(+15)	26	917	2.67(14)	3.90(15)
10	49.4	5.21(+17)	8.93(+14)	6.62(+15)	50	914	2.47(14)	1.70(15)
10	49.2	5.24(+17)	8.46(+14)	6.64(+15)	29	907	2.30(14)	2.68(15)
10	35.2	3.73(+17)	9.22(+14)	6.63(+15)	43	910	1.80(14)	2.30(15)
10	35.2	3.72(+17)	9.41(+14)	6.90(+15)	34	913	1.93(14)	2.63(15)
20	15.1	1.16(+17)	2.23(+14)	1.80(+15)	38	1258	9.13(14)	8.23(15)
20	15.2	1.18(+17)	2.31(+14)	1.84(+15)	43	1247	1.13(15)	1.01(14)
20	21.3	1.67(+17)	2.42(+14)	1.78(+15)	55	1231	9.70(14)	8.20(15)
20	21.4	1.68(+17)	2.41(+14)	1.84(+15)	46	1225	9.78(14)	1.04(14)
20	50.7	4.03(+17)	5.66(+14)	4.28(+15)	22	1215	9.32(14)	3.17(15)
20	50.7	4.03(+17)	5.72(+14)	4.34(+15)	17	1209	1.12(15)	8.91(15)
10	53.2	4.24(+17)	7.41(+14)	5.21(+15)	14	1212	6.41(14)	3.97(15)
10	50.9	4.02(+17)	6.71(+14)	4.86(+15)	15	1224	7.63(14)	3.13(15)
10	31.7	2.47(+17)	4.05(+14)	3.02(+15)	21	1236	7.64(14)	7.67(15)
10	31.7	2.46(+17)	4.01(+14)	2.99(+15)	20	1241	8.98(14)	5.83(15)
10	31.8	2.45(+17)	6.21(+15)	4.56(+15)	12	1233	7.11(14)	3.08(15)
10	31.8	2.44(+17)	6.24(+14)	4.59(+15)	12	1238	7.30(14)	1.91(15)
20	30.0	3.96(+17)	6.87(+14)	5.14(+15)	80	733	1.11(15)	1.32(15)
20	30.1	4.01(+17)	6.99(+14)	5.25(+15)	49	723	2.39(14)	2.83(15)
20	40.5	5.48(+17)	9.11(+14)	4.08(+15)	18	713	1.70(14)	9.01(16)
20	41.6	5.67(+17)	9.14(+14)	4.04(+15)	41	708	1.66(14)	9.18(16)
10	11.8	3.72(+17)	9.48(+14)	7.70(+14)	44	705	1.69(14)	9.88(16)
10	11.8	3.70(+17)	9.74(+14)	7.33(+15)	36	707	9.32(14)	7.22(16)
10	31.0	1.53(+17)	9.34(+14)	6.83(+15)	24	701	8.33(14)	1.13(15)
10	31.0	1.53(+17)	8.99(+14)	6.76(+15)	24	700	7.73(14)	8.99(16)

10	40.7	7.91(+17)	1.98(+15)	1.58(+16)	22	6	495	1.07(+15)	1.32(+16)
20	41.1	7.76(+17)	2.08(+15)	1.48(+16)	10	6	511	1.97(+15)	1.59(+16)
20	41.0	7.66(+17)	2.08(+15)	1.48(+16)	8	6	517	2.00(+15)	1.49(+16)
20	49.8	9.11(+17)	2.04(+15)	1.45(+16)	7	6	527	2.90(+15)	1.95(+16)
20	54.3	1.07(+18)	2.42(+15)	1.90(+16)	5	5	490	2.22(+15)	1.97(+16)
20	55.9	1.07(+18)	2.17(+15)	1.71(+16)	5	5	504	2.73(+15)	1.65(+16)
20	56.1	1.06(+18)	2.09(+15)	1.66(+16)	9	6	511	2.67(+15)	1.61(+16)
20	17.3	2.01(+17)	5.80(+14)	1.27(+15)	55	22	835	1.90(+14)	2.04(+15)
20	29.2	3.43(+17)	5.19(+14)	1.14(+15)	64	22	825	1.95(+14)	2.73(+15)
20	29.3	3.46(+17)	5.35(+14)	4.16(+15)	36	22	817	1.70(+14)	1.76(+15)
10	27.1	3.18(+17)	4.85(+14)	3.80(+15)	32	24	826	2.08(+14)	3.84(+15)
20	29.2	3.44(+17)	5.34(+14)	4.13(+15)	25	22	819	1.92(+14)	3.25(+15)
10	13.3	1.16(+17)	4.19(+14)	3.24(+15)	22	28	1106	7.02(+14)	7.22(+15)
20	11.3	9.85(+16)	3.68(+14)	2.79(+15)	16	35	1107	9.61(+14)	1.05(+14)
20	21.5	1.89(+17)	4.25(+14)	3.08(+15)	20	30	1096	6.08(+14)	4.32(+15)
20	21.5	1.90(+17)	4.16(+14)	3.11(+15)	12	29	1090	6.25(+14)	4.10(+15)
20	27.1	2.45(+17)	4.05(+14)	3.11(+15)	20	30	1080	5.82(+14)	3.54(+15)
20	27.5	2.46(+17)	4.14(+14)	3.14(+15)	18	30	1081	5.19(+14)	3.51(+15)
10	27.6	2.44(+17)	3.92(+14)	3.07(+15)	15	31	1090	8.95(+14)	9.62(+15)
10	27.7	2.45(+17)	3.90(+14)	3.01(+15)	14	31	1092	7.27(+14)	7.05(+15)
20	20.3	3.45(+17)	1.28(+15)	9.91(+15)	10	9	367	2.80(+15)	4.10(+16)
20	20.6	3.24(+17)	1.10(+15)	9.34(+15)	10	10	615	3.57(+15)	3.40(+16)
20	20.5	3.12(+17)	1.48(+15)	8.91(+15)	10	10	652	4.56(+15)	5.70(+16)
20	32.9	1.89(+17)	1.11(+15)	8.39(+15)	16	11	649	5.59(+15)	3.76(+16)
20	32.9	1.85(+17)	1.10(+15)	8.44(+15)	12	11	651	5.15(+15)	4.89(+16)
20	15.6	6.79(+17)	1.50(+15)	1.16(+16)	9	8	648	6.22(+15)	3.34(+16)
20	15.9	6.81(+17)	1.52(+15)	1.18(+16)	8	8	647	6.76(+15)	3.63(+16)
20	28.8	1.88(+17)	3.99(+14)	2.76(+15)	5	33	1180	1.80(+15)	1.05(+14)
20	28.9	1.89(+17)	3.67(+14)	1.53(+15)	2	35	1177	2.25(+15)	1.80(+14)
20	20.1	1.41(+17)	3.57(+14)	2.88(+15)	18	35	1171	1.91(+15)	1.68(+14)
20	20.3	1.45(+17)	3.77(+14)	2.78(+15)	29	35	1171	2.26(+15)	1.46(+14)
10	20.6	1.41(+17)	3.70(+14)	2.82(+15)	15	35	1188	2.48(+15)	2.59(+14)
10	20.6	1.41(+17)	3.78(+14)	2.84(+15)	24	35	1189	1.87(+15)	1.29(+14)
10	20.7	1.41(+17)	3.45(+14)	2.78(+15)	25	35	1189	2.06(+15)	1.46(+14)
10	29.5	1.90(+17)	3.45(+14)	2.70(+15)	20	34	1188	1.96(+15)	1.54(+14)
10	27.1	1.78(+17)	3.45(+14)	2.86(+15)	18	36	1181	2.13(+15)	1.94(+14)
20	15.0	7.19(+16)	2.25(+14)	1.65(+15)	85	57	1744	1.54(+15)	6.29(+14)
20	15.9	7.15(+16)	2.16(+14)	9.37(+15)	45	57	1747	9.25(+15)	6.97(+14)
20	16.7	9.09(+16)	2.75(+14)	1.15(+15)	29	46	1740	5.25(+15)	4.99(+14)
10	15.9	1.10(+15)	3.16(+14)	1.11(+15)	52	57	1744	1.29(+15)	3.29(+14)

Copy available as NTC does not
 produce

TABLE I (continued)
 Summary of Rate Coefficient Measurements of $\text{MCl} + \text{O} \rightarrow \text{Products}$

Oxidant Inlet Position (cm)	P (Torr)	[M] (cm^{-3})	$[\text{O}_2]$ Range (cm^{-3})	F_{O_2}	v (m s^{-1})	T (K)	k ($\text{cm}^3 \text{ molecule}^{-1} \text{ s}^{-1}$)	σ
10	19.9	1.10(+17)	3.51(+11)	1.42(+15)	37	1740	3.79(15)	3.33(14)
10	28.5	1.57(+17)	3.30(+11)	1.34(+15)	39	1740	2.88(15)	1.78(14)
10	28.1	1.56(+17)	3.00(+11)	1.36(+15)	39	1736	3.01(15)	2.83(14)
20	41.7	2.83(+17)	5.79(+14)	2.38(+15)	22	1523	1.81(15)	9.11(+15)
20	41.8	2.86(+17)	6.04(+14)	2.35(+15)	24	1511	1.90(15)	8.68(+15)
10	45.1	2.89(+17)	5.91(+14)	4.52(+15)	28	1507	1.03(15)	8.78(+15)
10	11.9	8.74(+16)	1.67(+14)	1.41(+15)	62	1649	3.30(13)	2.83(14)
20	11.9	8.73(+16)	1.66(+14)	1.37(+15)	41	1649	7.33(13)	5.37(14)
20	11.9	8.74(+16)	1.67(+14)	1.33(+15)	40	1650	7.06(13)	5.78(14)
10	23.8	1.40(+17)	4.14(+14)	2.93(+15)	77	1612	2.10(15)	1.81(14)
10	24.0	1.41(+17)	3.94(+14)	3.10(+15)	51	1637	2.11(15)	1.75(14)
20	17.5	1.70(+17)	3.49(+14)	2.79(+15)	244	998	1.88(11)	3.80(15)
20	17.5	1.69(+17)	3.57(+14)	2.77(+15)	207	999	5.27(11)	4.21(15)
20	22.6	2.18(+17)	8.28(+14)	3.68(+15)	109	1000	1.51(11)	3.77(15)
20	22.6	2.17(+17)	8.32(+14)	3.79(+15)	43	1002	3.91(11)	2.81(15)

a) The measurements are reported in the sequence in which they were obtained.

b) $1 \text{ Torr} = 133.3 \text{ Pa}$.

c) Arbitrary units.

AN HT FFR KINETICS STUDY OF THE REACTION BETWEEN AlCl AND CO₂ FROM 1175 TO 1775 K

Donald F. ROGOWSKI and Arthur FONTIJN

Department of Chemical Engineering, Rensselaer Polytechnic Institute, Troy, NY 12180-3590, USA

Received 24 September 1986

Rate coefficients for the reaction $\text{AlCl} + \text{CO}_2 \rightarrow \text{OAlCl} + \text{CO}$ have been measured in a high-temperature fast-flow reactor (HT FFR). These fit the expression $k(T) = 2.5 \times 10^{-12} \exp(-7550 \text{ K}/T) \text{ cm}^3 \text{ molecule}^{-1} \text{ s}^{-1}$. The existence of a large energy barrier for this exothermic reaction is in agreement with that suggested for the OAlCl channel of the $\text{AlCl} + \text{O}_2$ reaction. The presence of such barriers is in sharp contrast to the AlO reactions with CO_2 and O_2 .

1. Introduction

The use of the HT FFR technique is providing a data base for the kinetics of homogeneous gas-phase oxidation reactions of metallic species in the 300–1900 K range; results have been summarized in several reviews [1–3]. Following measurements of Al atom and AlO radical reactions, we recently initiated work on the AlCl radical with a study of its reaction with O_2 [4]. Here we report results for



and compare its $\ln k(T)$ versus T^{-1} behavior to that established in the $\text{AlCl} + \text{O}_2$ study and for the AlO reactions with CO_2 [5] and O_2 [6].

2. Experimental

The basic HT FFR design and methodology has been described previously [2]. The modifications used for AlCl measurements have been discussed elsewhere [4]. Briefly, a vertical 2.2 cm inner diameter mullite reaction tube is heated by silicon carbide rod-type heating elements. The reaction tube and heating elements are housed inside an insulated vacuum can. An Al-wetted tungsten coil is heated in the upstream end of the reaction tube producing gaseous Al. Ar bath gas with a trace ($\approx 5 \times 10^{12} \text{ cm}^{-3}$) of Cl_2 is passed over the coil. Al atoms are entrained and react at near gas

kinetic rates [7] to produce AlCl. Further downstream CO_2 is introduced through a movable inlet; the distance between it and the observation plane varies from 20 to 10 cm. Relative AlCl concentrations are measured at the observation plane by laser-induced fluorescence (LIF), using the $A-X(0, 0)$ transition at 261.4 nm. To ensure that AlCl production ceases at the CO_2 introduction point, some O_2 ($\approx 5 \times 10^{13} \text{ cm}^{-3}$) is added through the CO_2 inlet to consume any remaining free Al by the fast $\text{Al} + \text{O}_2$ reaction ($k \approx 3 \times 10^{-11} \text{ cm}^3 \text{ molecule}^{-1} \text{ s}^{-1}$ [6]). The gases used, are 99.5% Cl_2 , 99.998% Ar (from liquid), 99.6% O_2 , and 99.99% CO_2 , all obtained from Linde.

3. Results

Plots of $\ln [\text{AlCl}]_{\text{relative}}$ versus $[\text{CO}_2]$ yield straight lines with slopes $k_1 t$, where t is reaction time. k_1 at each experimental condition is determined by using a weighted linear regression of the data. The random experimental errors are used to determine the weighting by a propagation of errors method [2]. From this treatment the σ_{k_1} associated with each k_1 is calculated.

Below about 1175 K reaction (1) has been found to be too slow to allow meaningful HT FFR observation. Fifty-nine measurements of k_1 between 1175 and 1775 K have been made. Of these the fifty-four which have correlations $r > 0.85$ for $\ln [\text{AlCl}]_{\text{relative}}$

Table 1
Summary of rate coefficient measurements of $\text{AlCl} + \text{CO}_2 \rightarrow \text{OAlCl} + \text{CO}$ ^{a)}

Oxidant inlet position	\bar{P} (Torr) ^{b)}	$[\bar{M}]$ (10^{17} cm^{-3})	$[\text{CO}_2]$ range (cm^{-3})	\bar{v} (m s^{-1})	F ^{c)}	\bar{T} (K)	k ^{d)}	σ ^{d)}
20	19.7	1.24	1.03(15)–8.85(15)	40	49	1538	3.93(–14)	4.14(–15)
20	19.6	1.24	1.07(15)–9.07(15)	40	46	1533	3.84(–14)	3.21(–15)
20	24.6	1.56	1.03(15)–8.50(15)	42	28	1529	1.04(–14)	1.42(–15)
20	24.6	1.56	1.04(15)–8.26(15)	42	24	1526	1.30(–14)	1.48(–15)
20	32.8	2.07	1.37(15)–1.10(16)	31	31	1526	1.39(–14)	8.35(–16)
20	39.4	2.49	1.62(15)–1.30(16)	26	25	1527	1.04(–14)	1.01(–15)
10	34.2	2.18	1.72(15)–1.37(16)	25	26	1517	1.19(–14)	2.23(–15)
10	34.2	2.18	1.87(15)–1.36(16)	25	32	1514	1.25(–14)	2.51(–15)
20	23.0	1.55	1.17(15)–9.76(15)	35	34	1433	1.27(–14)	1.46(–15)
20	23.0	1.56	1.25(15)–1.00(16)	35	33	1423	9.60(–15)	9.10(–16)
20	23.7	1.62	1.18(15)–8.59(15)	39	22	1416	1.17(–14)	1.49(–15)
20	23.7	1.62	1.06(15)–8.62(15)	39	23	1414	9.25(–15)	1.08(–15)
10	26.5	1.80	1.24(15)–9.68(15)	35	25	1417	8.37(–15)	1.17(–15)
10	26.6	1.81	1.24(15)–9.63(15)	35	25	1418	9.37(–15)	9.92(–16)
10	20.0	1.35	1.28(15)–9.67(15)	35	41	1424	9.70(–15)	1.55(–15)
10	20.0	1.36	1.26(15)–1.00(16)	35	40	1425	1.24(–14)	2.22(–15)
20	25.7	1.87	1.62(15)–1.21(16)	29	36	1325	3.49(–15)	6.95(–16)
20	25.7	1.88	1.52(15)–1.20(16)	29	36	1320	4.75(–15)	9.77(–16)
20	37.0	2.73	2.27(15)–1.76(16)	20	14	1307	2.82(–15)	2.89(–16)
20	36.9	2.73	2.26(15)–1.74(16)	20	11	1304	2.77(–15)	4.63(–16)
20	19.9	1.47	1.07(15)–7.92(15)	43	54	1310	1.00(–14)	1.75(–15)
20	20.0	1.47	1.12(15)–8.02(15)	43	44	1311	1.04(–14)	1.32(–15)
20	20.0	1.46	1.06(15)–8.15(15)	43	43	1320	1.75(–14)	1.58(–15)
10	20.0	1.46	1.09(15)–8.14(15)	43	39	1322	1.95(–14)	3.32(–15)
20	31.5	1.91	1.38(15)–1.09(16)	31	17	1591	1.36(–14)	1.97(–15)
20	31.6	1.92	1.33(15)–1.13(16)	31	17	1587	1.29(–14)	1.17(–15)
10	31.6	1.91	1.36(15)–1.08(16)	31	12	1596	1.70(–14)	1.76(–15)
10	31.6	1.92	1.33(15)–1.13(16)	31	10	1592	1.18(–14)	2.60(–15)
20	31.5	1.91	1.63(15)–1.40(16)	25	40	1588	1.66(–14)	1.26(–15)
20	31.6	1.92	1.80(15)–1.40(16)	24	32	1586	1.60(–14)	1.42(–15)
10	31.5	1.91	1.82(15)–1.39(16)	25	41	1594	1.77(–14)	1.68(–15)
10	31.8	1.92	1.74(15)–1.40(16)	24	35	1593	1.91(–14)	1.40(–15)
20	22.1	1.25	1.12(15)–9.17(15)	37	40	1705	2.43(–14)	3.15(–15)
20	22.1	1.25	1.20(15)–9.09(15)	38	56	1703	1.84(–14)	1.26(–15)
10	22.1	1.25	1.19(15)–9.25(15)	38	55	1708	1.94(–14)	2.94(–15)
10	19.9	1.14	9.94(14)–8.47(15)	41	45	1689	3.79(–14)	5.91(–15)
20	20.4	1.17	7.80(14)–6.32(15)	55	24	1680	2.01(–14)	3.33(–15)
20	20.4	1.17	8.23(14)–6.41(15)	55	21	1679	1.53(–14)	3.10(–15)
20	16.9	0.924	7.24(14)–5.74(15)	60	55	1764	1.34(–13)	2.28(–14)
20	16.9	0.925	7.01(14)–5.68(15)	60	53	1762	1.01(–13)	6.75(–15)
10	27.1	1.50	1.38(15)–1.06(16)	32	58	1740	4.17(–14)	2.74(–15)
10	27.1	1.50	1.41(15)–1.07(16)	32	59	1745	2.88(–14)	3.14(–15)
20	19.1	1.05	8.28(14)–6.55(15)	53	121	1759	4.72(–14)	9.22(–15)
20	19.1	1.05	7.97(14)–6.64(15)	53	112	1756	4.88(–14)	4.93(–15)
10	19.1	1.06	8.34(14)–6.58(15)	52	82	1747	4.92(–14)	5.67(–15)
10	19.1	1.06	8.71(14)–6.60(15)	52	71	1739	4.74(–14)	5.74(–15)
10	32.9	1.84	1.35(15)–1.05(16)	33	39	1727	2.77(–14)	2.88(–15)
10	32.9	1.84	1.33(15)–1.02(16)	33	33	1726	3.04(–14)	3.31(–15)
20	31.4	2.55	1.87(15)–1.42(16)	24	35	1190	2.66(–15)	3.42(–16)
20	19.8	1.61	1.25(15)–9.14(15)	38	30	1190	1.32(–14)	1.55(–15)
20	19.8	1.61	1.18(15)–9.28(15)	38	49	1186	1.53(–14)	1.28(–15)
20	29.0	2.39	1.88(15)–1.36(16)	25	24	1175	7.09(–15)	7.52(–16)
20	22.6	1.67	1.28(15)–1.04(16)	34	23	1307	9.33(–15)	1.67(–15)
20	29.7	2.22	1.32(15)–1.01(16)	34	10	1291	1.01(–14)	1.85(–15)

a) The measurements are reported in the sequence in which they were obtained.

b) 1 Torr = 133.3 Pa. c) In arbitrary units. d) In $\text{cm}^3 \text{ molecule}^{-1} \text{ s}^{-1}$.

versus $[\text{CO}_2]$ are presented in table 1. Inspection of the data in table 1 shows k_1 to be independent of \bar{P} , $[\bar{M}]$ and the experimental parameters: inlet position, \bar{v} (the average gas velocity) and F (the initial fluorescence intensity, which is approximately proportional to the initial $[\text{AlCl}]$). It may also be seen that k_1 is independent of the position, which shows that the AlCl consumption measurements are not measurably influenced by quenching of AlCl(A) by CO_2 . Temperatures given are averages of the temperatures at 5 cm intervals from the CO_2 inlet position to the observation plane. The standard deviation about the mean gas temperature varied from ± 3 to ± 17 K depending on the reaction conditions. In view of systematic uncertainties in T [2], σ_T is taken as 25 K.

While at least some curvature may be expected in an Arrhenius plot covering a wide temperature range, within the scatter of the present results a normal Arrhenius expression $k = A \exp(-B/T)$ provides the best weighted least-squares fit [8] taking into account σ_{k_1} and σ_T . The resulting rate expression is

$$k_1(T) = 2.53 \times 10^{-12} \exp(-7550 \text{ K}/T) \quad (2)$$

$$\text{cm}^3 \text{ molecule}^{-1} \text{ s}^{-1}.$$

The standard deviation for $k_1(T)$ determined by a standard propagation of errors technique [8,9] is

$$\sigma_{k_1}(T) = k_1(T) [(\sigma_A/A)^2 + (\sigma_B/T)^2 - \sigma_{AB}/AT + (0.1)^2]^{1/2},$$

with variances and covariance

$$\sigma_A^2 = 4.08 \times 10^{-1} A^2,$$

$$\sigma_B^2 = 9.58 \times 10^5,$$

$$\sigma_{AB} = 6.21 \times 10^2 A.$$

In the determination of σ_{k_1} , the 0.1 is σ_n/n , the systematic uncertainty in the flow profile factor [2]. The covariance term $-\sigma_{AB}/AT$ must be taken into account in the determination of σ_{k_1} , since A and B are dependent parameters [9]. The resulting $2\sigma_{k_1}$ confidence levels are $\pm 23\%$ at 1175 K, $\pm 16\%$ at 1300 K, $\pm 12\%$ at 1550 K and $\pm 15\%$ at 1775 K. It should be noted that $\sigma_{k_1}(T)$ represents the uncertainty of the fitted expression, not the deviation of the measurements of k_1 .

4. Discussion

$\Delta H_R^0(298 \text{ K})$ for reaction (1), as written, is $-14 \pm 22 \text{ kJ mol}^{-1}$ [10]. Other product channels would be at least some 750 kJ mol^{-1} endothermic and do not need to be considered in the temperature range investigated. The 490 to 1750 K HT FFR study of the reaction



showed a strongly concave upward Arrhenius-type plot and yielded a rate coefficient expression [4]

$$k_2(T) = 1.3 \times 10^{-12} \exp(-3400 \text{ K}/T)$$

$$+ 3.4 \times 10^{-9} \exp(-16100 \text{ K}/T)$$

$$\text{cm}^3 \text{ molecule}^{-1} \text{ s}^{-1}.$$

Since neither OAlCl nor AlO_2 have identified electronic transition spectra, LIF could not be used for positive channel identification. However, arguments were advanced in that work, which suggest that the first term in the $k_2(T)$ expression essentially describes the behavior of channel (3b) and the second term that of reaction (3a). The second term becomes dominant only above 1650 K. Since it is thus determined over a narrow temperature interval it has a large associated uncertainty. However, this term clearly involves an activation energy well in excess of the 28.3 kJ mol^{-1} of the first term. Such a large activation energy for a simple exothermic abstraction reaction ($\Delta H_R^0(298 \text{ K}) = -47 \text{ kJ mol}^{-1}$ [10]) is somewhat unexpected. The $k_1(T)$ expression derived in the present work shows that there is a considerable barrier for OAlCl formation from AlCl and thus tends to strengthen the interpretation of the study of reaction (3). An HT FFR mass spectrometer apparatus is currently being constructed and should allow direct product identification.

HT FFR studies of



showed slightly negative T dependences of their rate coefficients from 500 to 1300 K [5] and 300 to 1400

K [6], respectively. Replacing the O atom in AlO with a Cl atom thus appears responsible for the appearance of major barriers in the reaction potential energy surfaces.

Acknowledgement

This work was supported under grant AFOSR-86-0019.

References

- [1] A. Fontijn and R. Zellner, in: Reactions of small transient species, kinetics and energetics, eds. A. Fontijn and M.A.A. Clyne (Academic Press, New York, 1983) ch. 1.
- [2] A. Fontijn and W. Felder, in: Reactive intermediates in the gas phase. Generation and monitoring, ed. D.W. Setser (Academic Press, New York, 1979) ch. 2.
- [3] A. Fontijn, *Combustion Sci. Technol.* 50 (1986) 151.
- [4] D.F. Rogowski and A. Fontijn, in: Twentv-First Symposium (International) on Combustion (The Combustion Institute, Pittsburgh), to be published.
- [5] D.F. Rogowski, A.J. English and A. Fontijn, *J. Phys. Chem.* 90 (1986) 1688.
- [6] A. Fontijn, W. Felder and J.J. Houghton, in: Sixteenth Symposium (International) on Combustion (The Combustion Institute, Pittsburgh, 1977) p. 871.
- [7] D.F. Rogowski and A. Fontijn, work in progress.
- [8] P.R. Bevington, *Data reduction and error analysis for the physical sciences* (McGraw-Hill, New York, 1969) ch. 11.
- [9] W.E. Wentworth, *J. Chem. Educ.* 42 (1965) 96.
- [10] JANAF Thermochemical Tables, Data sheets available in September 1986, Dow Chemical Co.

THE RADIATIVE LIFETIME OF $\text{AlCl}(A^1\Pi)$

Donald F. ROGOWSKI and Arthur FONTIJN

Department of Chemical Engineering, Rensselaer Polytechnic Institute, Troy, NY 12180-3590, USA

Received 10 February 1987, in final form 17 March 1987

The radiative lifetime of the $\text{AlCl}(A^1\Pi)$ state has been determined by a laser-induced fluorescence method to be 6.4 ± 0.5 ns. The estimated accuracy limits are $\pm 4\%$.

1. Introduction

Few radiative lifetime data on refractory species are currently available, compare e.g. Suchard [1] and Huber and Herzberg [2]. We are making kinetic measurements involving such species in a high-temperature fast-flow reactor (HTFFR) using laser-induced fluorescence (LIF). Recently, AlCl oxidation reactions [3,4] have been studied by observing the $\text{AlCl}(A^1\Pi-X^1\Sigma^-)$ (0,0) transition. Since no previous radiative lifetime studies of $\text{AlCl}(A^1\Pi)$ appear to have been made, we have now extended our work to provide this information.

Preliminary experiments showed that the 17.5 ns fwhm of the laser pulse and the 10 ns resolution of the signal recording equipment somewhat exceed the AlCl radiative lifetime, τ . The first difficulty has been addressed by Good et al. [5], whose approach is used here, see section 2. In section 3 we discuss the implications of using Good's technique with the 10 ns resolution of the recording equipment.

2. Technique

AlCl is produced in an HTFFR by the reaction of trace quantities of Al and Cl₂ in Ar, as described elsewhere [3,4]. A pulsed Lambda Physik EMG 101 excimer/FL 2002 dye laser with a KDP doubling crystal and coumarin 344 dye is used to induce the fluorescence. The $\text{AlCl}(A-X)$ (0,0) transition at 261.4 nm or the $\text{Al}(5^2S_{1/2}-3^2P_{1/2})$ transition at 265.2 nm

is used for fluorescence excitation and observation. The fluorescence radiation passes through a 262 ± 13 nm (fwhm) interference filter and is measured with an EMI 9813QA photomultiplier tube (PMT) with a 2.2 ns rise time. The output of the PMT is sent to a Data Precision Analogic 6000/620 100 MHz transient digitizer via a LeCroy VV100BTB wideband pulse amplifier. Fluorescence intensity, laser pulse and background measurements are made following established procedures [6,7]. For the measurement of the laser pulse, AlCl production is terminated and a scattering rod is placed in the laser beam. By adjusting the rod, the scattered laser radiation intensity can be made comparable to the fluorescence intensity. The background signal is then obtained by removing the rod. For each measurement, an average of 1000 pulses is used.

The fluorescence decay constant τ is evaluated from $f(t)$, the fluorescence signal with background subtracted, and $e(t)$, the laser pulse with background subtracted, by the iterative convolution method of Good et al. [5]. A τ is guessed and using this value $e(t)$ is convoluted with the response function, $h(t, \tau) = \exp(-t/\tau)$, to obtain $f'_d(t)$, the fluorescence signal anticipated to be observed for a response with the guessed value of τ . $f(t)$ and $f'_d(t)$ are normalized to their maximum value and the summation

$$\text{LSQ} = \sum_{i=1}^N [f(t_i) - f'_d(t_i)]^2 / f'_d(t_i)$$

is evaluated and then minimized by successive approximations for τ . In an attempt to reduce the

error associated with the numerical convolution to obtain $I_f(t)$, a 1 ns step size is used rather than the 10 ns step size of the digitizer. To achieve this, values for $e(t)$ at 1 ns increments are obtained by linear interpolation from the 10 ns data. After the convolution, only $I_f(t)$ at the 10 ns resolution of $I(t)$ are used in minimizing LSQ.

3. Results and discussion

Fig. 1 shows typical fluorescence, laser and background measurements for the AlCl experiments. The results of applying the iterative convolution method [5] to these data is shown in fig. 2. For comparison, the laser pulse and a synthetic fluorescence signal with $\tau = 10$ ns are also shown there.

Thirty measurements of τ for AlCl were made over a wide variety of experimental conditions. These are presented in table 1 and have an average value of 4.5 ns. To arrive at the radiative lifetime, τ_r , from this τ , two factors need to be considered. The first is quenching as expressed by

$$\tau^{-1} = \tau_r^{-1} + \sum_{i=1}^N k_{qi}[X_i],$$

where k_{qi} is the quenching rate coefficient for species

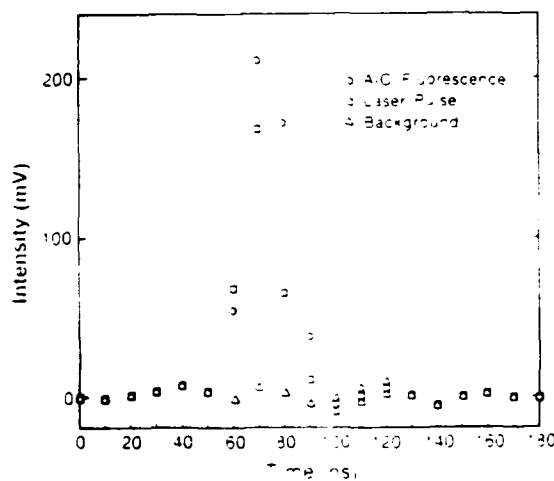


Fig. 1. Plot of experimental data. For $50 \leq t \leq 130$ ns the AlCl fluorescence intensity, laser pulse and background data are indistinguishable.

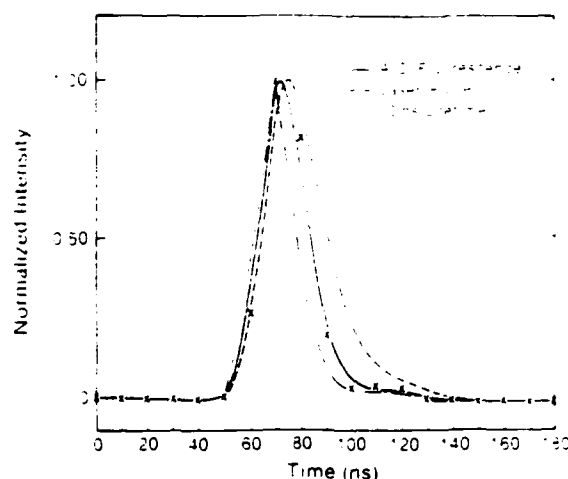


Fig. 2. Normalized plots of (i) the least-squares fit of the AlCl fluorescence signal and (ii) the laser pulse, both derived from fig. 1, with the background subtracted. Individual data points shown are for the observed fluorescence intensity. Also shown is the decay expected for $\tau = 10$ ns.

i and $[X_i]$ its concentration. For Cl_2 , if a maximum $k_{q\text{Cl}_2} = 3 \times 10^{-10} \text{ cm}^3 \text{ s}^{-1}$ is assumed and the maximum $[\text{Cl}_2]$ of $8 \times 10^{12} \text{ cm}^{-3}$ is used, $\tau^{-1}/k_{q\text{Cl}_2}[\text{Cl}_2] = 9 \times 10^4$. Hence quenching by Cl_2 is insignificant. The same argument also holds for AlCl since the maximum possible $[\text{AlCl}]$ is twice the maximum $[\text{Cl}_2]$. It should be noted though that $[\text{AlCl}]$ is estimated to be in the range 10^{10} to 10^{11} cm^{-3} . Within the scatter of the data no quenching of AlCl(A) by Ar is observed, see table 1. This is as expected since the maximum $[\text{Ar}]$ is $4 \times 10^{17} \text{ cm}^{-3}$ and $k_{q\text{Ar}}$ has been found to be typically less than $10^{-15} \text{ cm}^3 \text{ s}^{-1}$ for other electronically excited species, see e.g. refs. [8-10], which leads to $\tau^{-1}/k_{q\text{Ar}}[\text{Ar}] \geq 6 \times 10^5$. Thus quenching effects are negligible.

The second factor is that the τ determined is smaller than the 10 ns resolution of the digitizer. To determine the influence that this may have on τ , a computational test was made. Test fluorescence decays, $I_h(t, \tau)$, were generated by analytically convoluting a test excitation function, $e_h(t)$ with the response function, $h(t, \tau)$. The fwhm of $e_h(t)$ is 17.5 ns, the measured fwhm of the laser pulse. The values for $e_h(t)$ are (t in ns): $e_h(t) = 0$ for $t < 0$ (i.e. before the laser pulse); $e_h(t) = t/17.5$ for $0 \leq t \leq 17.5$; $e_h(t) = 2 - t/17.5$ for $17.5 \leq t \leq 35$; $e_h(t) = 0$ for $35 < t$. τ equal to 5, 10, and 15 ns were used with the

Table 1
AlCl(A ¹Π, v=0) decay constant measurements

P (Torr)	[Ar] (cm ⁻³)	[Cl ₂] (cm ⁻³)	T (K)	τ ^a (ns)	τ̄ (ns)
12.4	9.08(-16)	3.76(-12)	1316	4.6, 4.3, 4.1, 4.2, 4.7	4.4
24.6	1.53(-17)	7.51(-12)	1296	4.3, 4.5, 4.3, 4.3, 4.4	4.4
23.8	1.94(-17)	4.56(-12)	1186	4.8, 4.6, 4.6, 4.5, 4.4	4.6
34.9	3.99(-17)	3.57(-12)	1173	4.1, 3.8, 3.9, 3.9, 4.1	4.0
19.9	2.16(-17)	1.11(+13)	891	4.8, 5.0, 4.9, 4.7, 4.8	4.8
28.6	3.11(-17)	1.63(-13)	887	4.6, 4.3, 4.8, 4.7, 4.5	4.6

τ̄ = 4.5 (±2σ = 0.6) ns

^a 1 Torr = 133.3 Pa.

Table 2
Test radiative lifetime data

Time after start of laser pulse (ns)	τ _{cal} (ns)		
	τ _{cal} = 5.0 ns	τ _{cal} = 10	τ _{cal} = 15.0 ns
0.0	2.7	8.4	14.2
2.5	2.8	9.0	14.6
5.0	3.1	9.5	15.6
7.5	2.8	8.5	14.7
τ̄ _{cal} (ns)	2.9	8.9	14.8

response function. To mimic the 10 ns resolution of the digitizer, $f_b(t, \tau)$ and $e_b(t)$ were divided into four groups, starting at 0, 2.5, 5, and 7.5 ns after $e_b(t)$ becomes non-zero, with successive data points 10 ns apart. The test data were then analyzed as if it were experimental data. The results of this test are given in table 2.

Examination of table 2 shows that as the τ used to generate the test data, τ_{cal} , decreases from 15 to 5 ns, the τ determined by analysis of the data, τ_{cal} , is increasingly underestimated. Applying a linear

regression to the 5 and 10 ns results yields $\tau_{cal} = \frac{1}{2}\tau_{cal} + 2.6$ ns. This correction when applied to the experimental results yields $\tau_r = 6.4$ ns.

As a check on the data collection and analysis procedures, τ_r of Al 5 ²S_{1/2} was measured and found to be 20.8 ns, see table 3. Within the scatter of the data no quenching of excited Al by Ar is observed. The observed lifetime is larger than 15 ns, thus as may be seen from table 2 no correction to this value is necessary. τ_r for Al 5 ²S_{1/2} agrees within experimental error with the recommendation of Wiese et al. [11], who give a value of 25.2 ns with an estimated accuracy of ±25% and the LIF work of Jönsson and Lundberg [6], who give 24 ± 4 ns. Based on this comparison of Al values we conservatively assign a ±40% accuracy to τ_r AlCl(A ¹Π, v=0).

Finally, it is interesting to note that the value of τ_{rad} of AlCl(A ¹Π) is considerably shorter than that of the isoelectronic species BCl(A ¹Π), for which a τ_{rad} of 19.1 ± 2.0 ns has been reported [1,12].

Table 3
Al 5 ²S_{1/2} decay constant measurements

P (Torr)	[Ar] (cm ⁻³)	T (K)	τ (ns)	τ̄ (ns)
20.6	1.62(-17)	1230	20.7, 21.2, 21.1, 21.1, 21.2	21.1
33.9	2.70(-17)	1211	21.0, 20.5, 20.4, 20.4, 20.3	20.5
12.0	1.02(-17)	1134	21.0, 20.8, 20.8, 20.5, 20.7	20.8
29.9	2.58(-17)	1118	20.8, 20.7, 20.7, 20.8, 20.5	20.7

τ̄ = 20.8 (±2σ = 0.6) ns

Acknowledgement

We thank Dr. M.C. Heaven of Emory University for helpful comments and Dr. J.R. Fuhr of the NBS Data Center on Atomic Transition Probabilities for supplying the information on $Al\ 5^2S_{1/2}$. This work was supported under grant AFOSR-86-0019.

References

- [1] S.N. Suchard, Spectroscopic data (IFI Plenum Press, New York, 1975).
- [2] K.P. Huber and G. Herzberg, Molecular spectra and molecular structure, Vol. 4, Constants of diatomic molecules (Van Nostrand Reinhold, New York, 1979).
- [3] D.F. Rogowski and A. Fontijn, in Twenty-First Symposium (International) on Combustion (The Combustion Institute, Pittsburgh), to be published.
- [4] D.F. Rogowski and A. Fontijn, Chem. Phys. Letters 132 (1986) 413.
- [5] H.P. Good, A.J. Kallir and U.P. Wild, J. Phys. Chem. 88 (1984) 5435.
- [6] G. Jönsson and H. Lundberg, Z. Physik A313 (1983) 151.
- [7] J.N. Demas, Excited state lifetime measurements (Academic Press, New York, 1983) ch. 4.
- [8] P.H. Tennyson, A. Fontijn and M.A.A. Clyne, Chem. Phys. 62 (1981) 71.
- [9] F.R. Burden, M.A.A. Clyne and A. Fontijn, Chem. Phys. 65 (1981) 123.
- [10] K. Schofield, J. Phys. Chem. Ref. Data 8 (1979) 723.
- [11] W.L. Wiese, M.W. Smith and M.B. Miles, NSRDS-NBS 22, Vol. 2 (1969) p. 48.
- [12] J.E. Hesser, J. Chem. Phys. 48 (1968) 2518.

AN HTFFR KINETICS STUDY OF THE REACTION BETWEEN BCl AND O₂ FROM 540 TO 1670 K

Aleksandar G. SLAVEJKOV, Donald F. ROGOWSKI and Arthur FONTIJN

Department of Chemical Engineering, Rensselaer Polytechnic Institute, Troy, NY 12180-3590, USA

Received 19 October 1987

A method for the production of BCl in flow systems has been developed and used for the study of the title reaction in a high-temperature fast-flow reactor (HTFFR). The temperature dependence of the rate coefficients is described by the expression $k(T) = 2.2 \times 10^{-11} \exp(-4620 \text{ K}/T) \text{ cm}^3 \text{ molecule}^{-1} \text{ s}^{-1}$, consistent with a single reaction mechanism for the given temperature range. These $k(T)$ values are larger than those observed for the isoelectronic $\text{AlCl} + \text{O}_2$ and $\text{BF} + \text{O}_2$ reactions.

1. Introduction

The kinetics of homogeneous gas-phase oxidation reactions of several metallic species have been investigated over wide temperature ranges using the HTFFR technique [1-4]. We have now initiated studies of boron species. The first measurements concern the reaction of BCl with O₂ from 540 to 1670 K. We compare its $\ln k(T)$ versus T^{-1} behavior to that of the AlCl/O_2 [4] and the BF/O_2 [5] reactions. There are apparently no previous studies of the kinetics of BCl reactions.

2. Technique

The basic measurements and procedures followed here have been described previously [3,4]. The reactor has been slightly modified for the production of BCl. It is shown schematically in fig. 1. A vertical reaction tube is heated by SiC resistance heating elements inside an insulated vacuum housing. In the present work a mullite (McDanel MV 30) and a quartz (Finkenbeiner-GE semiconductor grade) reaction tube have been used. A number of conceptually promising methods for producing steady measurable concentrations of BCl have been investigated here. Only one led to consistent results and was used for this work: the production of BCl by passing Ar containing 10 to 30 ppm (v/v) B₂H₆ and

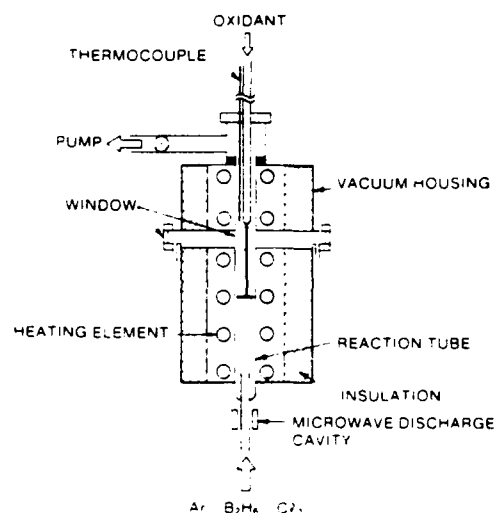


Fig. 1. Schematic of the HTFFR.

10 to 240 ppm (v/v) Cl₂ through a microwave discharge. The oxidant O₂ is introduced through a movable inlet system of the same material as the particular reaction tube. Oxidant inlet-to-window plane distances of 10 and 20 cm are used. A small flow of argon is introduced with the O₂ to improve the response time to changes in [O₂].

The relative concentration of the BCl is measured by laser-induced fluorescence using the A¹Π-X¹Σ⁺(0,0) transition at 272.0 nm. The frequency-doubled radiation of a Lambda Physik EMG 101

Table 1
Summary of rate coefficient measurements of the BCl + O₂ reaction

Oxidant inlet position (cm)	\bar{P} (Torr) ^{a)}	[M] (10 ¹⁶ cm ⁻³)	[O ₂] range (10 ¹⁴ cm ⁻³)	\bar{v} (m s ⁻¹)	$F^{b)}$	\bar{T} (K)	$k^{c)}$	$\pm \sigma^{d)}$
20	18.9	23.2	3.67-28.5	25	79	785	9.55	0.90
20	18.9	22.9	4.35-28.8	25	80	796	10.90	1.03
10	18.9	23.0	4.18-28.7	25	164	794	7.91	1.17
10	18.9	23.0	4.00-30.1	25	181	794	6.83	0.76
10	12.0	14.4	2.44-18.5	40	208	799	9.10	1.37
10	12.0	14.4	2.58-17.8	21	221	806	9.35	1.08
20	12.0	14.2	2.47-18.3	41	99	817	7.71	0.91
20	12.0	14.0	2.63-18.0	41	104	825	8.35	1.26
20	10.9	9.98	1.81-13.7	53	123	1051	31.5	3.52
20	10.9	9.92	1.83-13.9	53	107	1057	37.0	4.03
10	10.9	9.96	1.79-14.5	52	167	1056	25.3	3.08
10	10.9	9.87	1.82-13.9	53	159	1064	29.7	3.39
10	10.9	9.83	1.64-14.0	53	142	1068	31.1	3.93
10	10.9	9.76	1.85-13.8	54	150	1077	33.6	3.79
20	10.9	8.57	1.67-11.9	61	50	1224	49.8	5.85
20	10.9	8.55	1.83-11.8	60	45	1226	57.0	6.85
10	10.8	8.59	1.60-12.2	61	68	1218	53.8	6.07
10	10.8	8.59	1.67-11.7	61	65	1218	55.5	6.19
10	13.3	10.6	1.31-9.03	81	69	1207	37.1	3.89
10	13.3	10.6	1.31-8.88	81	73	1215	50.6	4.80
20	13.4	10.5	1.47-9.01	81	57	1225	59.8	5.04
20	13.4	10.5	1.19-8.90	82	54	1225	63.2	5.18
20	20.4	13.9	1.17-9.43	62	79	1412	96.0	6.85
20	20.4	13.9	0.77-6.20	62	95	1419	124.0	8.80
10	20.4	14.0	1.57-11.5	62	111	1412	85.9	8.85
10	20.4	14.0	1.80-11.7	61	103	1410	80.8	6.76
10	16.3	11.2	1.22-9.45	77	67	1409	84.5	7.27
10	16.4	11.1	1.25-9.45	77	59	1418	79.1	6.39
20	16.3	11.0	1.16-9.07	78	57	1430	85.1	6.32
20	16.4	11.1	1.22-9.32	78	51	1431	80.2	6.08
10	11.8	6.83	0.83-5.43	70	10	1662	161	27.1
10	13.3	7.72	1.12-7.84	93	18	1660	145	14.3
10	13.4	7.81	1.21-7.74	92	19	1658	179	17.6
10	16.5	9.61	1.01-7.39	99	43	1656	139	11.6
10	16.5	9.63	1.13-7.72	99	47	1651	172	13.0
20	15.3	8.84	0.80-6.87	108	41	1668	117	10.6
20	15.3	8.85	1.08-6.84	107	36	1665	118	10.8
20	14.0	12.9	1.81-14.3	53	70	1044	22.3	2.42
20	13.9	12.9	1.95-13.5	53	74	1042	25.4	2.16
10	14.0	12.8	1.74-14.2	53	133	1060	19	2.36
10	14.0	12.7	1.99-13.7	53	139	1064	23.2	2.44
10	31.2	29.2	2.36-18.4	40	201	1029	19.2	2.38
10	31.1	29.0	2.27-18.2	41	214	1032	21.7	1.90
20	26.6	25.1	1.95-15.8	47	136	1020	32.0	1.95
20	26.6	25.1	2.15-15.5	47	147	1021	31.2	2.41
20	12.6	13.5	2.71-19.1	38	58	904	8.74	0.994
20	12.6	13.5	2.80-19.6	38	74	900	13.0	1.43
10	12.6	13.4	2.53-19.3	38	116	908	8.56	1.07
10	12.6	13.4	2.73-19.2	38	110	912	9.71	1.36
10	20.7	22.3	2.35-18.0	41	218	896	9.26	0.912

Table 1 (continued)

Oxidant inlet position (cm)	\bar{P} (Torr) ^{a)}	$[M]$ (10^{17} cm ⁻³)	$[O_2]$ range (10^{14} cm ⁻³)	\bar{v} (m s ⁻¹)	$F^{b)}$	\bar{T} (K)	$k^{c)}$	$\pm \sigma^{d)}$
10	20.7	22.4	2.44-18.3	41	214	891	9.29	0.902
20	20.7	22.8	2.40-18.1	40	116	879	17.8	1.21
20	20.7	22.6	2.87-17.8	41	119	885	16.9	1.08
20	12.6	17.5	3.25-24.8	30	101	696	3.93	0.435
20	12.6	17.6	3.12-25.4	30	107	689	4.26	0.524
10	12.6	17.6	3.55-24.9	30	120	693	3.60	0.563
10	12.6	17.8	3.39-26.0	30	133	683	4.16	0.528
10	15.8	22.7	3.47-23.6	31	151	673	3.06	0.745
10	15.8	22.6	3.31-23.0	32	120	675	3.44	0.405
20	7.6	7.23	1.85-14.7	50	54	1008	26.3	4.20
20	7.5	7.26	2.07-12.0	50	51	1003	25.8	4.14
10	7.6	7.30	2.12-14.5	49	77	1002	19.1	3.13
10	7.6	7.32	2.18-14.9	49	76	1000	19.4	3.20
20	11.2	17.8	12.3-59.8	42	40	610	1.07	0.122
20	11.2	17.8	12.3-58.0	42	41	611	1.14	0.195
10	11.2	18.4	12.9-58.8	41	39	591	0.65	0.109
10	11.3	18.2	13.1-61.8	42	37	599	1.19	0.164
10	27.8	45.6	17.7-78.6	30	40	588	1.16	0.290

^{a)} The measurements are reported in the sequence in which they were obtained.

^{b)} 1 Torr = 133.3 Pa. ^{c)} In arbitrary units. ^{d)} In 10^{-14} cm³ molecule⁻¹ s⁻¹.

excimer/FL 2002 dye laser is used to pump this transition. The fluorescence is observed through a 270 nm (24 nm fwhm) interference filter. The gases used are Ar (99.999%, UHP) from the liquid, O₂ (99.6%, zero grade), Cl₂ (high-purity grade and 1.01% in Ar, custom grade) all from Linde, and diborane (1.08% in Ar, semiconductor grade) from Matheson.

3. Results

Plots of $\ln [BCI]_{\text{relative}}$ versus $[O_2]$ for fixed reaction zone lengths yield straight lines with slopes $-kt$, where t is the reaction time. k at each experimental condition is determined by using a weighted linear regression [2,4]. From this treatment the σ_k associated with each k is calculated. Experimental data are obtained from 540 to 1670 K. Below about 540 K the BCI fluorescence signals are too weak and unstable to allow meaningful observations.

Sixty-eight k measurements have been made with the mullite and sixty with the quartz reaction tube. The data from the mullite tube experiments are given

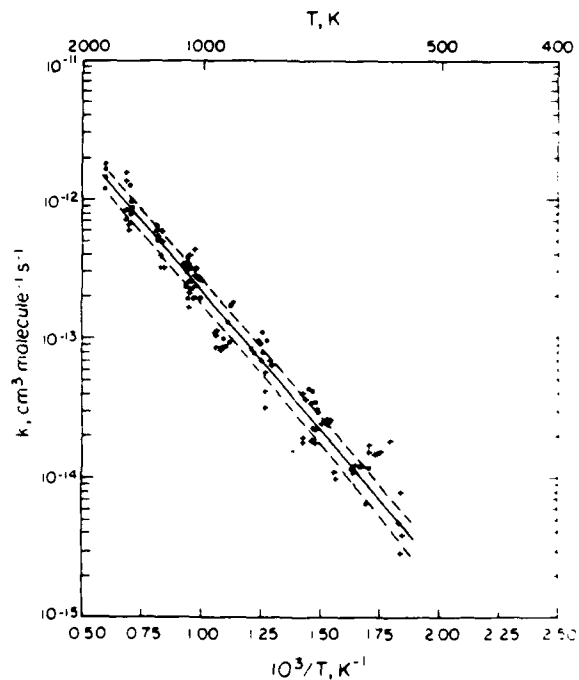


Fig. 2. Plot of the rate coefficients obtained for the BCI + O₂ reaction. ●, mullite reaction tube; +, quartz reaction tube.

in table 1. An Arrhenius type plot of these results along with the quartz tube data is shown in fig. 2. The two data sets are in agreement; the measurements made in the quartz tube are therefore not separately tabulated. It may be seen from table 1 that the values of k are independent of average total concentration $[M]$ varied from 7×10^{16} to 47×10^{16} cm^{-3} , average velocity \bar{v} varied from 13 to 107 m s^{-1} and F , the BCl fluorescence intensity at the lowest $[\text{O}_2]$ used. In addition k is independent of reaction zone length. Within the scatter of the data, fig. 2, no deviation from the normal Arrhenius equation $k(T) = A \exp(-B/T)$ is evident. A least-squares fit, weighted using σ_k and σ_T , yields

$$k(T) = 2.24 \times 10^{-11} \exp(-4620 \text{ K}/T) \quad (1)$$

$\text{cm}^3 \text{ molecule}^{-1} \text{ s}^{-1}$

with variance and covariances [3,4,6,7]: $\sigma_A = 7.35 \times 10^{-3} A^2$, $\sigma_B = 8.62 \times 10^3$, $\sigma_{AB} = 7.65 A$. For the fitting expression (1) the resulting $2\sigma_k(T)$ confidence levels which include a 10% systematic error in the flow profile factor [2,8] vary from $\pm 27\%$ at 540 K to $\pm 21\%$ in the range 900–1670 K.

4. Discussion

Two paths should be considered for the observed reaction:



Both channels are spin allowed and exothermic with ΔH_{298}^0 values of -208 and -305 kJ mol^{-1} , respectively [9]. On the basis of the current information we cannot distinguish between these channels, though the magnitude of the pre-exponential in eq. (1) suggests the simple O-atom abstraction reaction (2) as the most likely path. By contrast, for the reaction of the isoelectronic species AlCl with O_2 a strongly curved Arrhenius plot was obtained, cf. fig. 3. That result has been tentatively attributed to a change in mechanism [4]. The linear Arrhenius plot obtained for the $\text{BCl} + \text{O}_2$ reaction thus appears to suggest that no change in dominant mechanism occurs over the temperature range investigated. Mass spectrometry experiments are planned to identify the

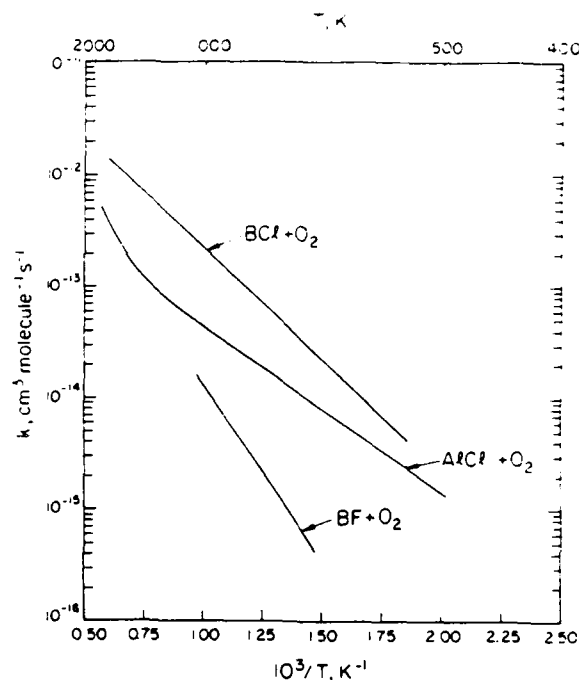


Fig. 3. Comparison of rate coefficients of the $\text{BCl} + \text{O}_2$ reaction to the $\text{AlCl} + \text{O}_2$ [4] and $\text{BF} + \text{O}_2$ [5] reactions.

products of both the BCl and AlCl reactions at a number of temperatures.

The $\text{BCl} + \text{O}_2$ reaction may be seen from fig. 3 to be faster than the $\text{AlCl} + \text{O}_2$ reaction over the temperature range investigated. Similarly, $\text{BCl} + \text{O}_2$ is at least an order of magnitude faster than the $\text{BF} + \text{O}_2$ reaction, which has been investigated from 675 to 1035 K by Light et al. [5]. Over that limited temperature range no deviation from a linear Arrhenius plot is evident for that boron halide reaction either.²

A more extensive comparison between B and Al radical oxidation kinetics is underway in our laboratory.

Acknowledgement

This work is supported under grant AFOSR-86-

² If we accept the lower limit value for the O-(AlO) bond of 530 kJ mol^{-1} from our work [1,10], then the dioxide and the oxyhalide product channels of the BCl, AlCl and BF reactions are all exothermic.

0019. We thank Dianne Rovero for technical assistance.

References

- [1] A. Fontijn, *Combustion Sci. Technol.* 50 (1986) 151.
- [2] A. Fontijn and W. Felder, in: *Reactive intermediates in the gas phase. Generation and monitoring*, ed. D.W. Setser (Academic Press, New York, 1979) ch 2.
- [3] D.F. Rogowski and A. Fontijn, *Chem. Phys. Letters* 132 (1986) 413.
- [4] D.F. Rogowski and A. Fontijn, Twenty-first Symposium (International) on Combustion (The Combustion Institute, Pittsburgh), to be published.
- [5] G.C. Light, R.R. Herm and J.H. Matsumoto, *J. Phys. Chem.* 89 (1985) 5066.
- [6] P.R. Bevington, in: *Data reduction and error analysis for the physical science* (McGraw-Hill, New York, 1969) ch 1.
- [7] W.E. Wentworth, *J. Chem. Educ.* 42 (1965) 96.
- [8] A. Fontijn and W. Felder, *J. Phys. Chem.* 83 (1979) 24.
- [9] M.W. Chase et al., *JANAF thermochemical tables*, 3rd Ed., *J. Phys. Chem. Ref. Data* 14 (1985) suppl. 1.
- [10] D.F. Rogowski, A.J. English and A. Fontijn, *J. Phys. Chem.* 90 (1986) 1688.

High-Temperature Fast-Flow Reactor Kinetics Studies of the Reactions of
Al with Cl₂, Al with HCl, and AlCl with Cl₂ over Wide Temperature Ranges

Donald F. Rogowski,[†] Paul Marshall, and Arthur Fontijn*

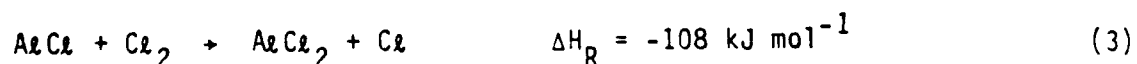
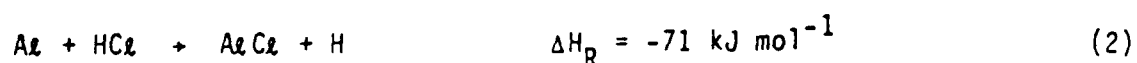
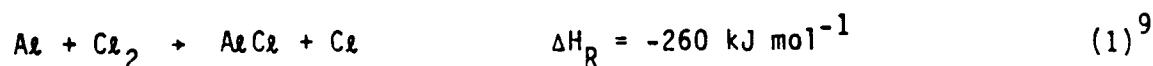
High-Temperature Reaction Kinetics Laboratory, Department of Chemical
Engineering, Rensselaer Polytechnic Institute Troy, New York 12180-3590

The HTFFR (High-Temperature Fast-Flow Reactor) technique has been used to measure rate coefficients for the title reactions under pseudo-first-order conditions. The relative concentrations of the minor reactants (Al-species) were monitored by laser-induced fluorescence. The following $k(T)$ expressions in $\text{cm}^3 \text{ molecule}^{-1} \text{ s}^{-1}$ are obtained: $\text{Al} + \text{Cl}_2 \rightarrow \text{AlCl} + \text{Cl}$, $k_1(T) = 7.9 \times 10^{-10} \exp(-780 \text{ K}/T)$ between 425 and 875 K; $\text{Al} + \text{HCl} \rightarrow \text{AlCl} + \text{H}$, $k_2(T) = 1.5 \times 10^{-10} \exp(-800 \text{ K}/T)$ between 475 and 1275 K; $\text{AlCl} + \text{Cl}_2 \rightarrow \text{AlCl}_2 + \text{Cl}$, $k_3(T) = 9.6 \times 10^{-11} \exp(-610 \text{ K}/T)$ between 400 and 1025 K. Confidence limits are given in the text. Indications are obtained that the expressions for $k_1(T)$ and $k_2(T)$ are approximately valid to at least 1300 and 1700 K, respectively. The results are discussed in terms of a harpooning mechanism and a modified form of collision theory, which takes account of long-range attractive potentials and conservation of angular momentum.

[†] Present Address: Westvaco Research Center, Covington, VA 24426

1. Introduction

The temperature dependence of the kinetics of oxidation reactions of metallic free radicals represents a little studied subject, of great practical importance.¹ Theoretical understanding and predictive ability are far less than for C/H/O/N type reactions,^{2,3} for which a still inadequate, but much larger, experimental data base is available. We are engaged in providing an extensive set of rate coefficient data for Al species. Earlier results on reactions of Al and AlO with oxygen oxidizers have been summarized.¹ Most recently, measurements on the reactions of AlCl with O₂ and CO₂ have been reported.^{4,5} Together these reactions show an interesting variety of $\ln k$ vs. T^{-1} relations, including approximately Arrhenius,⁵ zero or small negative activation energies,^{6,7} and concave upward, best approximated by double experimental expressions.^{4,8} Reasonable, if not always conclusive, a posteriori explanations for all these cases can be given.^{1,2,4-8} In the present work, this effort has been extended to include the reactions



Over the present temperature ranges these reactions show, within experimental error, no deviation from linear Arrhenius $\ln k(T)$ vs T^{-1} dependences.

2. Technique

The basic reactor design and methodology of the HTFFR technique have been discussed¹⁰ and details of the most recent design modifications have been

described.^{4,7,11} The reactor used here consists of a 60 cm long, 2.2 cm i.d. vertical mullite reaction tube, surrounded by resistance heating elements, contained in an insulated vacuum housing. It has a usable temperature range from about 400 to 1800 K. Upstream of the reaction zone free A_2 atoms are vaporized from an A_2 -wetted tungsten coil at about 1100 to 1300 K and are entrained in Ar bath gas. This coil can be resistance-heated directly from an independent power supply. For A_2C_2 reactant production a trace of C_2 , typically <0.005% of the Ar flow, is added to the bath gas. In earlier experiments it has been shown that this A_2C_2 formation takes place, at least in part, from reaction (1) in the gas-phase.⁴ Further downstream C_2 or HC_2 is introduced through a movable inlet, situated at 20 or 10 cm upstream from the observation plane. Relative A_2 and A_2C_2 concentrations at this plane are monitored by laser-induced fluorescence using a pulsed Lambda Physik EMG 101 excimer/FL 2002 dye/KDP doubling crystal combination, with coumarin 344 dye. A_2 is pumped and observed on the $5^2S_{1/2}-3^2P_{1/2}$ transition at 262.5 nm. For A_2C_2 the 261.4 nm A-X (0,0) transition is similarly used. To effectively remove interference from the hot reactor walls, a 262 nm, 13 nm FWHM filter is placed in front of the EMI 9813 QA photomultiplier tube for all these observations. The gases used are Ar from the liquid (99.998%) and C_2 (99.5%) through the bath gas inlet, and 1% C_2 (99.5%) in Ar (99.998%) or 5% HC_2 (99.995%) in He (99.999%) through the oxidant inlet.

Plots of $\ln[A_2]_{\text{relative}}$ or $\ln[A_2C_2]_{\text{relative}}$ versus $[C_2]$ or $[HC_2]$ for fixed reaction zone lengths (fixed oxidant inlet positions) yield straight lines with slopes $-kt$, where t is reaction time. k at each experimental condition is determined by a weighted linear regression.^{4,10,12} From this treat-

ment a σ_k associated with each k is found. The uncertainty in temperature is estimated as $\sigma_T = \pm 25$ K.^{4,5} The temperature dependences of the rate coefficients for reactions (1-3) are best described by the equation

$$k(T) = A \exp(-B/T) \quad (4)$$

The parameters for this fit expression are obtained using regression techniques, which account for σ_k and σ_T .^{11,12} Since A and B are dependent parameters, determination of the uncertainties of the fit requires the covariance σ_{AB} , as well as the variances σ_A^2 and σ_B^2 .¹³ Then, a standard deviation for the fit may be assigned,

$$\sigma_{k(T)} = k(T) [(\sigma_A/A)^2 - 2 \sigma_{AB}/AT + (\sigma_B/T)^2 + (0.1)^2]^{1/2} \quad (5)$$

In this expression, the term 0.1 represents σ_η/η , the assigned systematic uncertainty for the flow profile factor η .^{10,14} The resulting $\pm 2 \sigma_{k(T)}$ uncertainties are given in the figures showing the data for the individual reactions.

3. Results

The measured individual rate coefficients for reactions (1) through (3), and the conditions under which they were obtained, are given in Tables I through III, respectively. It may be seen that these rate coefficients are independent of $[\bar{M}]$ the average total concentration, \bar{P} the average pressure, \bar{v} , the average gas velocity and the oxidant inlet to observation plane distance, i.e., the observed reaction zone lengths of 10 or 20 cm.

The forty rate coefficient measurements for the $A_2 + Cl_2$ reaction (1) between 425 and 875 K give $k_1(T) = 7.85 \times 10^{-10} \exp(-779 \text{ K}/T) \text{ cm}^3 \text{ molecule}^{-1} \text{ s}^{-1}$ with associated variances and covariance, cf. eq. (4), $\sigma_A^2 = 2.31 \times 10^{-2} \times A^2$,

$\sigma_{AB} = 1.45 \times 10^1 \times A$, and $\sigma_B^2 = 9.45 \times 10^3$. For the $Al + HCl$ reaction (2) the fifty-three measurements from 475 to 1275 K result in $k_2(T) = 1.52 \times 10^{-10} \exp(-803 K/T) \text{ cm}^3 \text{ molecule}^{-1} \text{ s}^{-1}$, with $\sigma_A^2 = 1.21 \times 10^{-2} \times A^2$, $\sigma_{AB} = 8.98 \times A$, and $\sigma_B^2 = 7.24 \times 10^3$. For the $AlCl + Cl_2$ reaction (3) the sixty measurements spanning the 400 to 1025 K temperature range yield $k_3(T) = 9.56 \times 10^{-11} \exp(-613 K/T) \text{ cm}^3 \text{ molecule}^{-1} \text{ s}^{-1}$, with $\sigma_A^2 = 7.38 \times 10^{-3} \times A^2$, $\sigma_{AB} = 4.49 \times A$, and $\sigma_B^2 = 3.01 \times 10^3$.

The magnitudes of the rate coefficients obtained at the low pressures used in this investigation indicate that the reactions are bimolecular. The paths given in Eqs. (1) to (3) represent the only channels accessible from thermochemical considerations.⁹ Reaction (1) was used as the $AlCl$ production reaction for reaction (3), see Section 2, thus the LIF experiments on the latter reaction confirm $AlCl$ as a product species of the former.

A number of additional measurements were made¹¹ on reactions (1) and (2) at temperatures where the Cl_2 and HCl equilibrium dissociation exceeds 10%. These data were therefore not used in the above $k(T)$ calculations. However, no significant deviations from the extrapolated $k_1(T)$ were observed till about 1300 K. Further increases in temperature lead to a rapid decrease in k_1 values, indicative of Cl_2 dissociation. The k_2 measurements showed no such drop-off to 1715 K, the highest temperature investigated. It therefore is probable that the $k_1(T)$ and $k_2(T)$ expressions given are applicable at least up to these respective limits.

4. Discussion

The rate coefficients and the fit expressions are shown in Figs. 1 through 3. Within the scatter of the data, no definite curvature in the

Arrhenius plots can be detected. Since the rate coefficients, especially those of reaction (1), are close to gas kinetic, no sharp upward curvature with increasing temperature would have been expected.

There apparently have been no previous experimental measurements of reactions (1-3). However, a theoretical study by Mayer, Schieler and Johnston, who used a modified BEBO method, predicted $k_1(T) = 2.8 \times 10^{-13} T^{0.67} \exp(-6800 \text{ K}/T)$ and $k_2(T) = 5.5 \times 10^{-13} T^{0.67} \exp(-3900 \text{ K}/T) \text{ cm}^3 \text{ molecule}^{-1} \text{ s}^{-1}$, respectively.¹⁵ These values are several orders of magnitude lower than measured here and predict too strong a temperature dependence. While the BEBO approach has led to agreement with experimental data for some H-atom transfer reactions at 1000 K and above,^{15,16} for reactions involving metal atoms, such as Al , other approaches are needed.

4.1 Al -Atom Reactions (1) and (2)

The pre-exponential factor for reaction (2) is typical for atomic metathesis.^{17a} By contrast reaction (1) has a significantly larger pre-exponential, which is consistent with an electron-jump mechanism. The simple harpoon model¹⁸ predicts that electron transfer will occur at a separation r_c where

$$\text{IP}(\text{Al}) - \text{EA}(\text{C}_2) = e^2/4\pi\epsilon_0 r_c \quad . \quad (6)$$

Using values for the ionization potential IP of Al of 5.986 eV¹⁹ and for the vertical²⁰ electron affinity EA of C_2 of 1.02 eV,²¹ we calculate a reaction cross section $\sigma = \pi r_c^2$ of 0.26 nm². This is in accord with the mean cross section at the mid-point of the experimental temperature range, $\sigma = 0.28 \text{ nm}^2$.

An alternative interpretation of the Al -atom reactions can be based on collision theory. The reaction cross section from simple collision theory in

terms of the collision diameter d , the collision energy E_T and the energy threshold E_0 is²²

$$\begin{aligned} \sigma_{\text{SCT}} &= 0 & E_T < E_0 \\ &= \pi d^2 (1 - E_0/E_T) & E_T > E_0 \end{aligned} \quad (7)$$

In order to estimate d we take account of long-range attractive potentials of the form $V(r) = -C_6/r^6$. The maximum impact parameter b_{max} leading to collision is given by²²

$$b_{\text{max}}^2 = (3/2)^{2/3} (3 C_6/E_T)^{1/3} \quad (8)$$

Because b_{max}^2 is only weakly dependent on E_T we shall employ Plane and Saltzman's approximation and set d^2 equal to b_{max}^2 at the mean collision energy of the experiments.²³ Integration of Eq. (7) over a thermal energy distribution yields the standard result²²

$$k_{\text{SCT}}(T) = \pi d^2 (8k_B T/\pi u)^{1/2} \exp(-E_0/RT) \quad (9)$$

For reaction (1) C_6 is estimated via the Slater-Kirkwood expression:²⁴

$$C_6 = 2.48 \times 10^{-78} \alpha_1 \alpha_2 / [(\alpha_1/n_1)^{1/2} + (\alpha_2/n_2)^{1/2}] \text{ J m}^6 \quad (10)$$

where α_1 and α_2 are the polarization volumes for the reactants expressed in units of 10^{-24} cm^3 and n_1 and n_2 are the number of outer shell electrons. The α values for Al and Cl_2 ¹⁹ lead to $C_6 = 4.25 \times 10^{-77} \text{ J m}^6$ and hence $\pi d^2 = 0.87 \text{ nm}^2$. We fit E_0 to the experimental value of k_1 at 650 K and find $E_0 = 6.1 \text{ kJ mol}^{-1}$. With this value Eq. (9) agrees with the experimental fit to $k_1(T)$ to within 15% over the temperature range studied.

We may now apply this simple collision theory to reaction (2). In order

to calculate C_6 for a system involving dipole-induced dipole forces, these forces are taken into account by an additional term²⁵

$$C_6 = p^2 \alpha / 4\pi \epsilon_0 \quad \text{J m}^6 \quad (11)$$

where α is the polarizability volume of Ar and p the dipole moment of HCl . Equations (10) and (11) yield contributions to the total C_6 coefficient of 2.48×10^{-77} and $9.7 \times 10^{-79} \text{ J m}^6$, respectively. The resulting πd^2 is 0.67 nm^2 which would imply a pre-exponential factor from Eq. (9) about 5 times larger than observed for reaction (2). The discrepancy may be due to effects from conservation of angular momentum. González Ureña *et al.* have shown that among exothermic atom-diatom molecule reactions with low barriers, those which have a ratio of the reduced mass of the products to that of the reactants considerably smaller than 1 may have a reduced cross section and hence a rate coefficient smaller than predicted by Eq. (9).²⁶ For reaction (2) this ratio is 0.063. This can be contrasted to reaction (1) where this ratio is 1.2 and no angular momentum restrictions arise.²⁶

For the reaction heavy + heavy-light \rightarrow heavy-heavy + light the departing light atom carries little angular momentum. Conservation of angular momentum requires therefore that the initial orbital angular momentum of the reactants, which is equal to $(2\mu E_T b^2)^{1/2}$, is almost completely converted to product rotational angular momentum. Here μ is the reduced mass of the reactants and b is the impact parameter. The product angular momentum is $(2I' E_R')^{1/2}$, where I' is the moment of inertia of the diatomic product and E_R' is its rotational energy.^{26,27} The largest momentum-allowed impact parameter b_{max} is then given by $b_{\text{max}}^2 \sim I' E_{R',\text{max}}' / (\mu E_T)$. The maximum rotational energy $E_{R',\text{max}}'$ reflects

the energy disposal of the reaction. Here we shall assume $E'_{R,max} = \beta(E_T + Q)$ where Q is the reaction exothermicity and β is the fraction of the total available energy which is partitioned into rotation,²³ further assumed to be constant. Noting that $I' = \mu r^2$, where r is the equilibrium separation of the heavy-heavy product molecule i.e. A_2C_2 ,²⁷ we can derive a cross section σ_{AM} which is restricted by angular momentum:

$$\sigma_{AM} = \pi b_{max}^2 = \pi r^2 \beta (E_T + Q)/E_T \quad (12)$$

σ_{SCT} increases with increasing E_T whereas σ_{AM} decreases, so that the cross section σ reaches a maximum at a collisional energy E_{max} where

$$E_{max} = (d^2 E_0 + r^2 3Q)/(d^2 - 3r^2) \quad (13)$$

Thus

$$\begin{aligned} \sigma &= 0 & E_T < E_0 \\ &= \pi d^2 (1 - E_0/E_T) & E_0 < E_T < E_{max} \\ &= \pi r^2 \beta (1 + Q/E_T) & E_{max} < E_T \end{aligned} \quad (14)$$

Integrating this σ over a thermal distribution of E_T yields a rate coefficient k_{AM} that reflects the influence of angular momentum conservation:

$$k_{AM}(T) = k_{SCT}(T) - \left(\frac{8k_B T}{\pi \mu} \right)^{1/2} \times \left[\pi d^2 \frac{(RT + E_{max} - E_0)}{RT} - \pi r^2 \beta \frac{(RT + E_{max} + Q)}{RT} \right] \exp(-E_{max}/RT). \quad (15)$$

Qualitatively, it may be seen that if E_{max} is close to E_0 (i.e., β is small) $k_{AM}(T)$ will have a similar temperature dependence to $k_{SCT}(T)$ but a smaller pre-exponential factor.

We have calculated $k_{AM}(T)$ for the reaction $A_2 + HC_2$ using literature

values of $Q = 71 \text{ kJ mol}^{-1}$ and $r = 0.213 \text{ nm}$,⁹ and find agreement to within 5% of the experimental fit expression when $E_0 = 8.3 \text{ kJ mol}^{-1}$ and $\beta = 0.12$. These values correspond to $E_{\text{max}} = 10.4 \text{ kJ mol}^{-1}$. The value of β is consistent with an approximately linear transition state which imparts little torque to the departing AlCl . By contrast, the reaction $\text{Li} + \text{HCl}$ has a larger β of 0.3,^{23,28} an observation which is consistent with the bent transition state derived from ab initio calculations.²⁹ While the particular values of E_0 and β for reaction (2) are best determined by molecular beam techniques, this treatment illustrates that kinematic effects may have a significant influence on the magnitude of thermal rate coefficients.

4.2 AlCl Reaction (3)

The measured pre-exponential of reaction (3), $9.6 \times 10^{-11} \text{ cm}^3 \text{ molecule}^{-1} \text{ s}^{-1}$, is large compared to other metathesis reactions between diatomic reactants.^{17b} This factor, combined with the low activation energy, is consistent with there being a harpooning component to the mechanism: application of the electron-jump model used for reaction (1) with $\text{IP}(\text{AlCl}) = 9.4 \text{ eV}$ ⁹ yields $\sigma = 0.092 \text{ nm}^2$ at 700 K. The experimental value is similar but somewhat smaller, 0.060 nm^2 . We may further view the large pre-exponential of $k_3(T)$ in terms of the reverse reaction. The equilibrium constant is approximately $2.6 \exp(12700 \text{ K}/T)$ over the range 400 to 1000 K,⁹ which implies $k_{-3}(T) = 4 \times 10^{-11} \exp(-13300 \text{ K}/T)$. This pre-exponential factor is reasonable for an atomic metathesis.^{17a}

4.3 General Observations

Reactions (1) through (3) have large cross sections and are therefore suitable candidates for molecular beam studies, the results of which could permit a more quantitative collision theory interpretation of reactions (2)

and (3). Further theoretical development is also desirable to satisfactorily describe these reactions.

It is interesting to compare $k(T)$ for the $A_2 + C_2$ and $A_2 + HC_2$ reactions to the $k = 3.4 \times 10^{-11} \text{ cm}^3 \text{ molecule}^{-1} \text{ s}^{-1}$, independent of temperature from 300 to 1700 K, obtained for the $A_2 + O_2$ reaction.⁶ That reaction apparently goes through an intermediate complex, which preferentially dissociates to the original reactants.^{1,2,6} The positive temperature dependence of reactions (1) and (2), as well as their larger pre-exponentials, indicates that no such complex is formed in these C_2 -transfer reactions. Similarly, $k_3(T)$ may be compared to the $k(T)$ of the $A_2C_2 + O_2$ and $A_2C_2 + CO_2$ reactions of $1.3 \times 10^{-12} \exp(-3400 \text{ K}/T) + 3.4 \times 10^{-9} \exp(-16100 \text{ K}/T)$ from 490 to 1750 K⁴ and $2.5 \times 10^{-12} \exp(-7550 \text{ K}/T) \text{ cm}^3 \text{ molecule}^{-1} \text{ s}^{-1}$ from 1175 to 1775 K,⁵ respectively. All three reactions have positive temperature dependences, but the C_2 -transfer reaction (3) is, in the observed temperature regime, more than two orders of magnitude faster than the other two reactions.

Acknowledgements

This work is supported under grant AFOSR 86-0019, Dr. M.A. Birkan, technical monitor.

References

- (1) Fontijn, A. Combust. Sci and Tech., **1986**, 50, 151.
- (2) Fontijn, A.; Zellner, R. Reactions of Small Transient Species, Kinetics and Energetics, Fontijn, A.; Clyne, M.A.A., Eds.; Academic Press: London, **1983**, Chapter 1.
- (3) Gardiner, W.C., Jr., Ed. Combustion Chemistry, Springer-Verlag: New York, **1984**.

- (4) Rogowski, D.F.; Fontijn, A. Symp. (Int.) Combust., [Proc.] 21st, 1988, 943.
- (5) Rogowski, D.F.; Fontijn, A. Chem. Phys. Lett. 1986, 132, 413.
- (6) Fontijn, A.; Felder, W.; Houghton, J.J. Symp. (Int.) Combust., [Proc.] 16th 1977, 871.
- (7) Rogowski, D.F.; English, A.J.; Fontijn, A. J. Phys. Chem. 1986, 90, 1688.
- (8) Fontijn, A.; Felder, W. J. Chem. Phys. 1977, 67, 1561.
- (9) The thermochemical data used are obtained from Chase, M.W., Jr.; Davies, C.A.; Downey, J.R., Jr.; Frurip, D.J.; McDonald, R.A.; Syverup, A.N. JANAF Thermochemical Tables, J. Phys. Chem. Ref. Data 1985, 14.
- (10) Fontijn, A.; Felder, W. Reactive Intermediates in the Gas Phase. Generation and Monitoring, Setser, D.W., Ed.; Academic Press: New York, 1979, Chapter 2.
- (11) Rogowski, D.F., Ph.D. Thesis, Rensselaer Polytechnic Institute, 1988.
- (12) Bevington, P.R. Data Reduction and Error Analysis for the Physical Sciences, McGraw-Hill: New York, 1969, p. 242; Irvin, J.A.; Quickenden, T.I. J. Chem. Educ., 1983, 60, 711.
- (13) Wentworth, W.E. J. Chem. Educ., 1965, 42, 96.
- (14) Fontijn, A.; Felder, W. J. Phys. Chem., 1979, 83, 24.
- (15) Mayer, S.W.; Schieler, L.; Johnston, H.S. Symp. (Int.) Combust., [Proc.] 11th 1967, 837.
- (16) Mulcahy, M.F.R. Gas Kinetics, Nelson, London, 1973, Chapter 5; Zellner, R. in Ref. 3, Chapter 3.
- (17) Benson, S.W. Thermochemical Kinetics, 2nd Ed., Wiley, New York,

- (17) Benson, S.W. Thermochemical Kinetics, 2nd Ed., Wiley, New York, 1976, a) p. 148; b) p. 157.
- (18) Magee, J.L. J. Chem. Phys. 1940, 8, 687.
- (19) Weast, R.C.; Astle, M.J.; Beyer, W.H., Eds. CRC Handbook of Chemistry and Physics, 66th ed., CRC Press, Boca Raton, 1985.
- (20) Herschbach, D.R. Adv. Chem. Phys. 1966, 10, 319.
- (21) Ayala, J.A.; Wentworth, W.E.; Chen, E.C.M. J. Phys. Chem. 1981, 85, 768.
- (22) Smith, I.W.M. Kinetics and Dynamics of Elementary Gas Reactions, Butterworth London, 1980, Chapter 3.
- (23) Plane, J.M.C.; Saltzman, E.S., J. Chem. Phys. 1987, 87, 4606.
- (24) Pitzer, K.S. Adv. Chem. Phys. 1959, 2, 59.
- (25) Atkins, P.W. Physical Chemistry, 2nd Ed., W.H. Freeman, New York, 1978, Chapter 23.
- (26) González Ureña, A; Herrero, V.J.; Aoiz, F.J. Chem. Phys. 1979, 44, 81.
- (27) González Ureña, A; Adv. Chem. Phys. 1987, 66, 213.
- (28) Becker, C.H.; Casavecchia, P.; Tiedemann, P.W.; Valentini, J.J.; Lee, Y.T. J. Chem. Phys. 1980, 73, 2833.
- (29) Palmieri, P.; Garcia, E.; Laganá, A. J. Chem. Phys. 1988, 88, 181.

TABLE I

Summary of Rate Coefficient Measurements of $\text{Al} + \text{Cl}_2 \rightarrow \text{AlCl} + \text{Cl}^{\text{a}}$

Oxidant Inlet Position (cm)	\bar{P} (Torr) ^{b)}	$[\bar{M}]$ (10^{17} cm^{-3})	$[\text{Cl}_2]$ Range (10^{11} cm^{-3})	\bar{v} (m s^{-1})	\bar{T} (K)	k ($10^{-10} \text{ cm}^3 \text{ molecule}^{-1} \text{ s}^{-1}$)	$\pm \sigma$
20	20.2	3.73	3.64 - 25.1	31	524	1.50	0.10
20	20.2	3.67	3.03 23.8	32	532	1.76	0.14
10	20.3	3.74	3.20 24.4	31	523	2.52	0.18
10	20.3	3.72	2.92 24.8	32	527	2.70	0.21
10	18.2	3.27	2.26 17.6	44	539	2.88	0.24
10	18.3	3.26	2.09 18.4	45	541	2.89	0.24
20	18.3	3.20	2.38 17.4	45	552	2.02	0.15
20	18.3	3.23	2.10 17.0	45	543	2.15	0.15
20	27.1	3.77	3.52 24.8	32	694	2.07	0.13
20	27.1	3.77	3.38 24.3	32	693	1.85	0.16
10	27.1	3.80	3.50 23.4	32	689	2.31	0.17
10	27.1	3.80	3.16 24.6	32	688	3.11	0.19
10	23.0	3.07	2.12 16.6	47	724	2.58	0.24
10	23.1	3.11	2.01 16.9	47	715	3.07	0.19
20	23.1	3.12	2.08 17.7	47	714	2.60	0.19
20	23.1	3.14	2.13 17.0	47	710	2.40	0.19
20	22.2	2.48	1.70 14.3	58	864	2.95	0.16
20	22.3	2.53	1.62 13.8	57	849	2.85	0.17
10	22.3	2.57	1.60 13.6	57	839	4.32	0.38
10	23.1	2.66	1.66 13.8	55	839	3.85	0.27

10	14.9	1.69	1.75 - 15.3	52	848	3.17	0.30
10	14.9	1.68	1.80 15.0	52	852	3.51	0.35
20	14.9	1.67	2.06 15.1	53	857	2.90	0.24
20	14.9	1.67	1.87 14.9	53	861	3.06	0.26
20	12.3	1.74	2.44 20.0	41	683	2.18	0.21
20	12.3	1.73	2.38 19.7	42	688	2.26	0.21
10	12.3	1.81	2.45 20.3	40	657	2.21	0.24
10	12.4	1.82	2.52 20.2	40	655	2.36	0.26
10	23.1	3.46	2.70 18.6	42	643	2.30	0.18
10	23.1	3.49	2.68 18.5	42	639	2.36	0.22
20	23.1	3.49	2.50 18.9	42	639	1.82	0.13
20	23.1	3.51	2.37 19.9	42	635	1.93	0.14
20	22.9	5.12	3.24 29.8	29	431	.783	0.06
20	22.9	4.92	3.83 27.2	30	450	.934	0.10
10	23.0	4.97	3.45 27.2	30	446	1.13	0.10
10	23.0	4.92	2.95 28.4	30	451	1.36	0.12
10	16.4	3.56	2.39 18.4	41	446	1.38	0.12
10	16.5	3.50	2.42 18.0	42	455	1.71	0.21
20	16.5	3.36	2.22 17.9	44	474	1.51	0.12
20	16.5	3.38	2.23 18.8	44	472	1.37	0.11

a) The measurements are reported in the sequence in which they were obtained.

b) 1 Torr = 133.3 Pa

TABLE II

Summary of Rate Coefficient Measurements of $\text{Al} + \text{HCl} \rightarrow \text{AlCl} + \text{H}^{\text{a}}$

Oxidant Inlet Position (cm)	\bar{P} (Torr) ^{b)}	$[\bar{M}]$ (10^{17} cm^{-3})	[HCl] Range (10^{12} cm^{-3})	\bar{V} (m s^{-1})	\bar{T} (K)	k ($10^{-11} \text{ cm}^3 \text{ molecule}^{-1} \text{ s}^{-1}$)	$\pm \sigma$
20	12.1	2.43	1.05 - 9.11	44	481	2.41	0.25
20	12.4	2.39	.985 8.94	44	499	2.70	0.32
10	12.4	2.46	.919 8.95	43	486	4.16	0.56
10	12.4	2.43	1.18 8.94	44	492	3.65	0.48
10	20.2	3.90	1.42 10.3	37	500	3.21	0.37
10	20.2	3.94	1.50 11.0	36	495	3.00	0.37
20	20.2	3.97	1.51 10.9	36	492	2.09	0.25
20	20.2	3.97	1.45 10.9	36	492	2.03	0.15
20	30.2	3.48	1.18 9.40	41	836	3.50	0.24
20	30.2	3.50	1.13 9.67	41	832	3.52	0.28
10	30.2	3.53	1.14 9.54	40	827	3.96	0.36
10	30.3	3.55	1.36 9.96	40	822	6.83	0.56
10	16.0	1.86	1.40 10.7	37	833	5.30	0.62
10	16.0	1.84	1.37 10.4	38	841	5.83	0.51
20	16.0	1.82	1.36 9.80	38	850	6.66	0.58
20	16.0	1.81	1.30 10.7	38	849	6.34	0.55
20	20.5	2.67	1.31 9.38	40	742	5.22	0.37
20	20.5	2.68	1.46 9.77	39	739	4.88	0.37
10	20.5	2.71	1.27 9.53	39	732	5.87	0.15
10	20.6	2.71	1.47 9.70	39	731	5.72	0.47

10	28.9	3.86	1.13 - 9.80	37	722	5.55	0.44
10	28.9	3.88	1.47 10.1	37	718	5.72	0.45
20	28.9	3.83	1.35 10.4	38	729	3.59	0.37
20	28.9	3.83	1.37 10.4	38	729	3.30	0.32
20	25.3	3.92	1.25 11.3	37	623	3.12	0.19
20	25.3	3.91	1.29 11.2	37	625	3.12	0.28
10	25.4	3.91	1.24 9.67	37	627	4.28	0.42
10	25.4	3.92	1.35 10.8	37	626	4.62	0.39
10	18.3	2.80	1.04 7.74	52	630	5.66	0.79
10	18.3	2.75	.902 7.58	53	642	6.30	0.63
20	18.3	2.73	.897 7.23	53	646	4.61	0.37
20	18.3	2.74	1.03 7.84	53	644	4.64	0.32
20	15.7	1.43	.587 4.68	82	1061	9.07	0.91
20	15.7	1.43	.541 4.71	82	1059	9.75	0.66
10	15.7	1.44	.487 4.90	82	1053	8.66	0.88
10	15.7	1.44	.561 5.03	82	1055	9.62	0.87
10	24.6	2.26	.881 7.05	52	1053	7.24	0.10
10	24.6	2.26	.851 7.69	52	1053	8.39	0.72
20	24.6	2.27	.916 7.38	52	1045	7.44	0.71
20	24.6	2.26	1.06 7.09	52	1050	7.41	0.64
20	30.5	2.31	.920 8.06	51	1275	7.65	0.70
20	30.5	2.32	.879 7.40	51	1270	8.01	0.58
10	30.5	2.32	.935 8.43	51	1267	8.54	0.66
10	30.5	2.32	.937 7.69	51	1265	8.20	0.64
10	40.3	3.08	1.36 10.8	38	1262	7.26	0.58
10	40.3	3.09	1.45 10.1	38	1259	8.04	0.59

20	40.3	3.09	1.41 - 9.70	38	1257	6.40	0.50
20	40.7	3.11	1.44 9.24	38	1262	6.84	0.46
20	19.6	3.16	1.34 10.9	35	597	5.43	0.37
20	17.8	2.75	.980 7.82	48	625	5.25	0.41
20	17.9	2.79	1.05 8.11	48	617	5.30	0.40
10	17.8	2.78	.987 8.35	48	618	5.23	0.58
10	17.8	2.81	.966 8.19	48	610	4.20	0.48

a) The measurements are reported in the sequence in which they were obtained.

b 1 Torr = 133.3 Pa

TABLE III

Summary of Rate Coefficient Measurements of $\text{AlCl} + \text{Cl}_2 + \text{AlCl}_2 + \text{Cl}^{\text{a}}$

Oxidant Inlet Position (cm)	\bar{P} (Torr) ^{b)}	$[\bar{M}]$ (10^{17} cm^{-3})	$[\text{Cl}_2]$ Range (10^{11} cm^{-3})	\bar{v} (m s^{-1})	\bar{T} (K)	k ($10^{-11} \text{ cm}^3 \text{ molecule}^{-1} \text{ s}^{-1}$)	$\pm \sigma$
20	20.2	4.85	7.34 - 62.0	26	402	1.23	0.20
20	20.2	4.86	8.44 60.9	26	401	1.17	0.17
10	20.2	4.94	8.75 66.3	26	395	2.57	0.35
10	20.2	4.90	7.79 63.7	26	397	3.01	0.25
10	28.5	6.89	12.1 87.4	19	399	2.56	0.31
10	28.5	6.85	11.4 82.9	19	401	2.66	0.28
20	28.3	6.67	10.5 82.3	19	400	1.66	0.23
20	28.4	6.66	11.3 86.2	19	411	1.17	0.31
10	18.0	3.32	7.58 60.1	27	524	2.74	0.40
10	18.1	3.08	6.57 53.9	29	565	2.09	0.51
20	18.1	2.87	7.05 52.1	32	610	3.17	0.25
20	18.1	2.90	7.32 51.1	31	603	2.57	0.20
20	32.1	5.11	10.6 77.6	21	607	2.91	0.21
20	32.2	5.08	9.82 75.0	21	611	3.28	0.34
10	32.2	5.18	10.9 77.9	20	599	3.15	0.48
10	32.2	5.17	10.1 77.8	20	601	3.40	0.27
20	34.4	4.65	7.28 57.4	27	715	4.49	0.44
20	34.5	4.67	7.86 56.2	27	712	3.63	0.27
10	34.5	4.70	7.55 59.8	27	708	4.16	0.40
10	34.5	4.72	7.39 56.7	27	706	4.81	0.42

10	20.6	2.81	4.61 - 33.8	45	707	6.17	0.77
10	20.6	2.78	4.79 35.3	46	715	5.59	1.05
20	20.7	2.78	5.43 34.8	46	716	3.70	0.44
20	20.7	2.78	4.91 35.1	46	718	2.84	0.37
20	18.3	2.00	2.93 25.7	64	882	3.66	0.63
20	18.3	2.00	3.00 26.1	64	882	5.15	0.45
20	28.5	3.13	5.44 37.9	41	881	3.88	0.44
20	28.5	3.13	4.72 40.6	41	879	3.48	0.33
10	28.5	3.16	5.37 40.9	41	872	5.96	0.87
10	28.6	3.16	5.14 38.6	41	873	4.70	0.45
10	40.0	4.45	6.76 57.0	29	868	4.59	0.39
10	40.0	4.45	7.25 53.7	29	868	5.10	0.43
20	30.6	2.79	4.30 34.5	46	1061	5.91	0.45
20	30.7	2.83	4.35 34.5	46	1048	5.88	0.53
10	30.6	2.82	4.58 34.1	46	1045	5.95	0.52
10	30.7	2.84	4.25 35.2	46	1042	4.83	0.67
10	42.1	3.85	5.00 43.2	37	1055	7.26	0.71
10	42.3	3.92	5.52 42.4	36	1041	6.22	0.66
20	42.5	3.98	5.54 45.1	36	1031	5.06	0.32
20	42.5	3.99	5.11 44.4	36	1028	4.81	0.36
20	31.2	4.05	6.14 47.2	35	743	3.36	0.35
20	31.3	4.09	5.95 45.8	35	738	3.18	0.35
10	31.3	4.15	5.79 45.7	34	728	5.54	0.61
10	31.3	4.18	5.47 45.7	34	723	4.44	0.56
20	27.4	5.97	10.8 85.7	18	443	1.75	0.14
20	27.5	6.00	12.9 87.5	18	442	2.10	0.26

10	27.5	6.12	13.3 - 92.1	17	433	2.60	0.29
10	27.5	6.13	12.9 86.7	17	433	2.46	0.30
10	18.4	4.10	8.07 59.7	26	433	2.41	0.58
10	18.4	4.13	8.14 61.0	26	429	2.74	0.36
20	18.4	4.05	8.09 61.5	26	438	2.44	0.30
20	18.4	4.06	8.16 62.1	26	438	2.51	0.21
20	18.3	3.41	6.57 52.6	31	518	2.75	0.24
20	18.3	3.44	6.71 55.2	30	513	3.45	0.47
10	18.3	3.51	7.85 50.7	30	503	4.01	0.52
10	18.3	3.53	6.71 51.5	30	500	4.35	0.56
10	14.8	2.88	7.51 53.2	29	497	2.18	0.58
10	14.9	2.90	7.78 53.5	29	496	3.03	0.69
20	14.9	2.88	7.74 55.4	29	499	3.01	0.26
20	14.9	2.85	7.39 52.9	29	504	3.09	0.26

a) The measurements are reported in the sequence in which they were obtained.

b) 1 Torr = 133.3 Pa

Figure Captions

Fig. 1 Rate coefficient data for the Al/Cl_2 reaction

_____ Rate expression fit of the data given in text.

----- Two standard deviations to the fit of the rate expression as described in the text.

Fig. 2 Rate coefficient data for the Al/HCl reaction

_____ Rate expression fit of the data given in text.

----- Two standard deviations to the fit of the rate expression as described in the text.

Fig. 3 Rate coefficient data for the AlCl/Cl_2 reaction

_____ Rate expression fit of the data given in text.

----- Two standard deviations to the fit of the rate expression as described in the text.

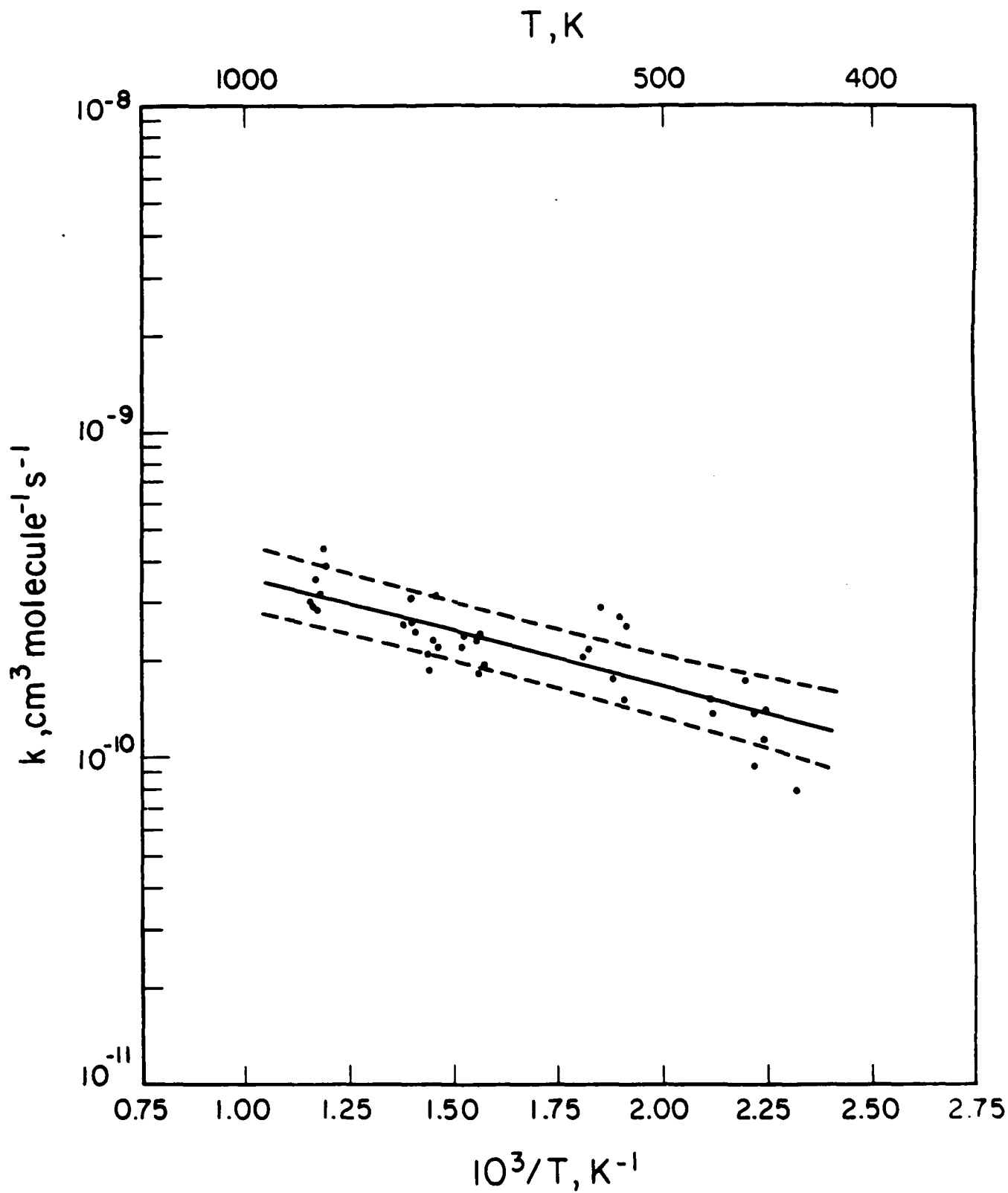


Figure 1

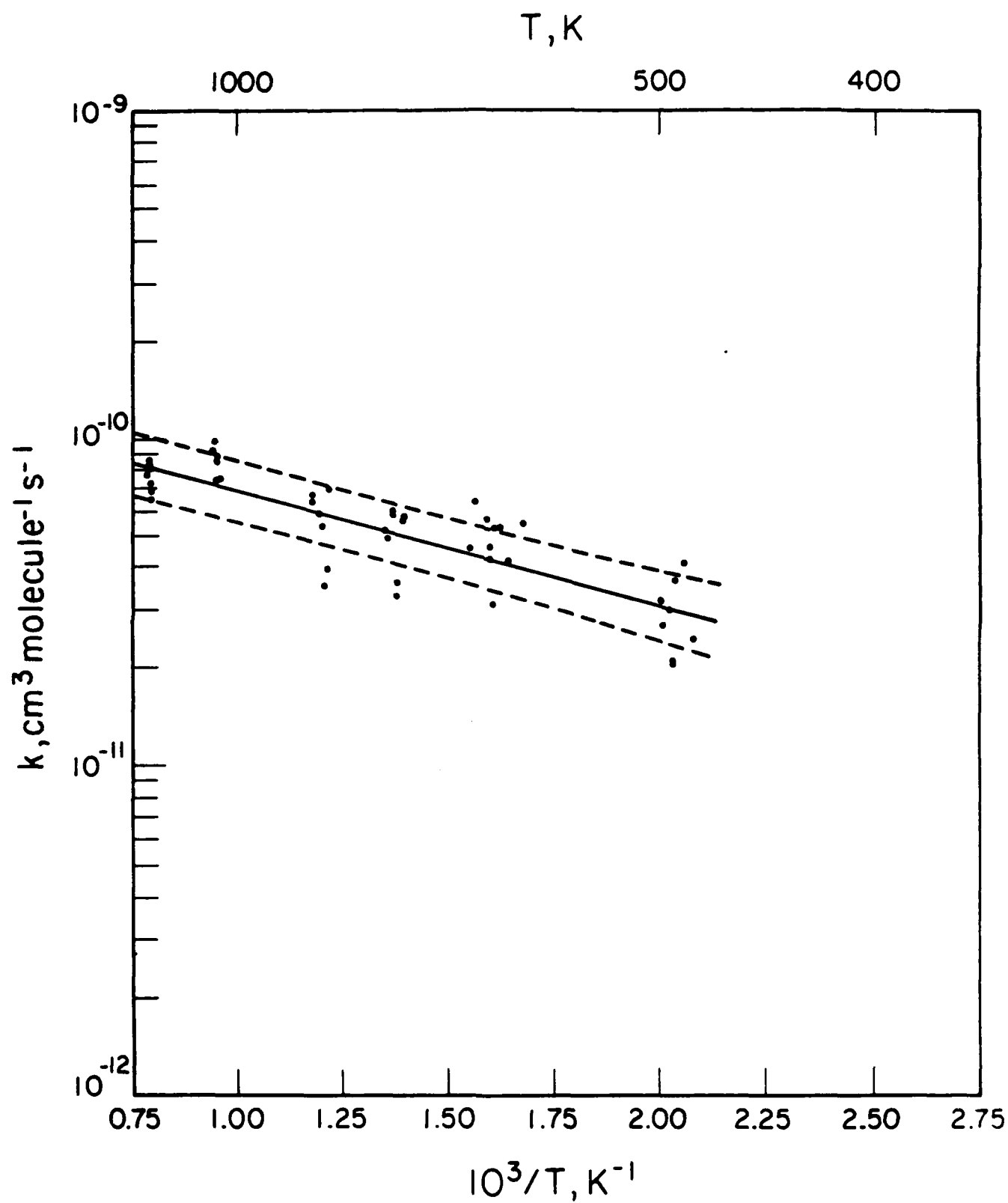


Figure 2

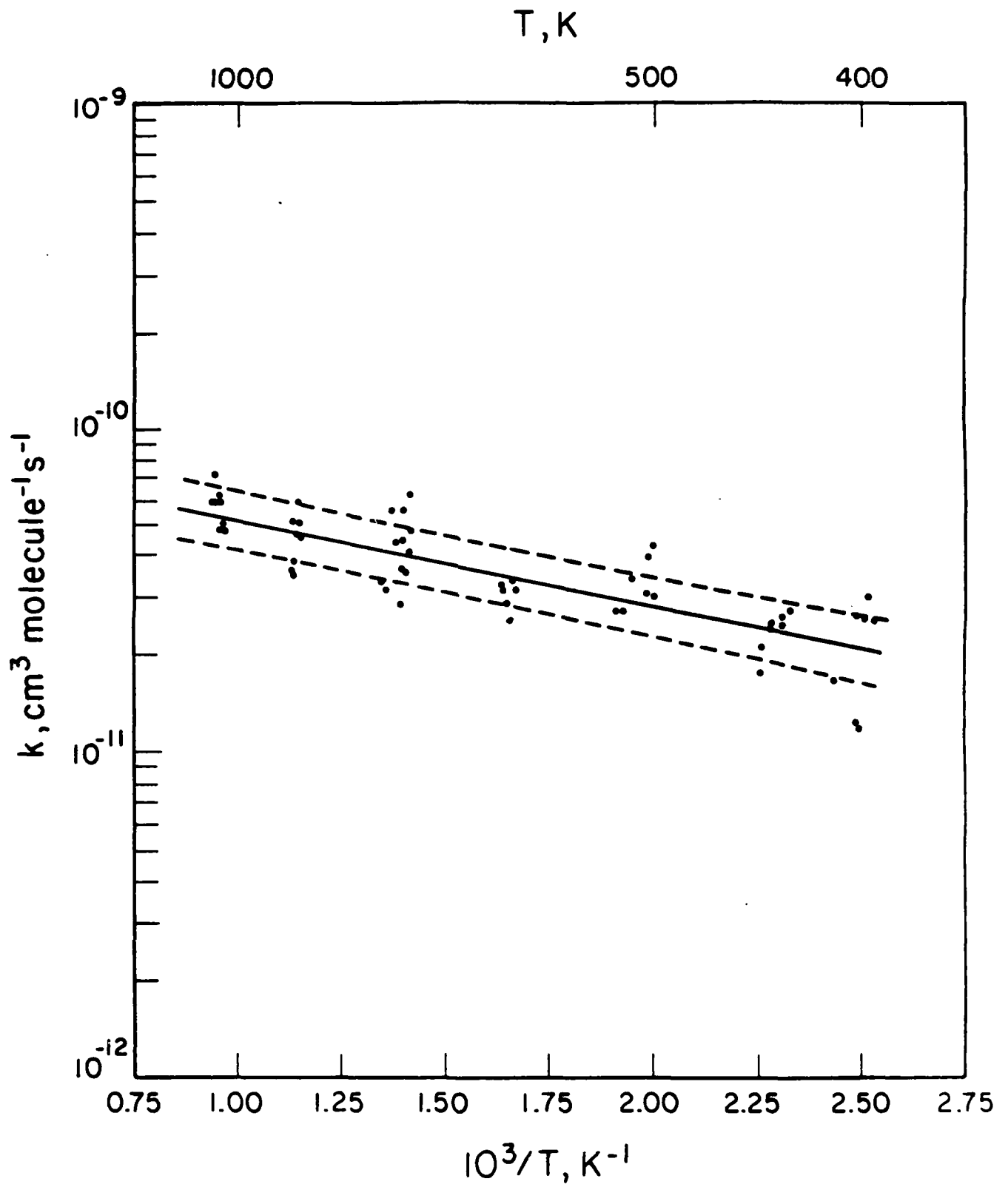


Figure 3